AMMONIA-WATER BINARY-VAPOUR POWER CYCLE - A CHOICE OF FUTURE

by

LOKESH KUMAR GARG

DEPARTMENT OF MECHANICAL ENGINEERING

INDIAN INSTITUTE OF TECHNOLOGY KANPUR

July, 1999

AMMONIA-WATER BINARY-VAPOUR POWER CYCLE - A CHOICE OF FUTURE

A Thesis Submitted

in Partial Fulfillment of the Requirements

for the Degree of

MASTER OF TECHNOLOGY

by

LOKESH KUMAR GARG

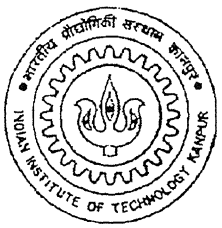

to the

DEPARTMENT OF MECHANICAL ENGINEERING

INDIAN INSTITUTE OF TECHNOLOGY KANPUR

JULY, 1999

Dedicated to

My Parents, Sisters and Brothers.

CERTIFICATE

It is to certify that the work contained in the thesis entitled **Ammonia-Water Binary-Vapour Power Cycle - A Choice of Future, by Lokesh Kumar Garg,** has been carried out under my supervision and that this work has not been submitted elsewhere for a degree.

12/7/99

Dr. Manohar Prasad
Professor
Department of Mechanical Engineering
Indian Institute of Technology, Kanpur

July, 1999

Acknowledgements

The author, with immense pleasure expresses his indebtness and a deep sense of gratitude to Dr. Manohar Prasad, whose devotion and encouragement at every step with active participation enabled me to carry out this modest piece of work. It has been a great pleasure to work under him.

The author, also takes this opportunity to pay his reverence to Dr. Keshav Kant for his constant encouragement.

Particular thanks are due to Mr. Ajit Kumar Shukla for his timely and valuable suggestions.

The author wishes to extend his gratitude to Mr.P. N. Mishra, Mr. R. C. Vishwakarma, Mr. R. V. Gujral for their help.

Finally the author wishes to thank his friends, in particular Vikas, Rahul, Rajkumar, Manoj, Lokesh Pathak, Alok, Gaurav, Vipin, Ashok for their cooperation and assistance throughout his stay at IITK.

Lokesh Kumar Garg

IIT Kanpur

July, 1999

Synopsis

Steam is mostly used in thermal power plants. It has negative condensing pressure below 373 K and high volume flow rate in low-pressure turbines. Binary-vapour cycle is used to overcome these deficiencies.

In the present work analysis of ammonia-water binary-vapour cycle has been carried out by developing thermodynamic functions using least square interpolations and by developing a computer program. Steam and ammonia are used in topping cycle and bottoming cycles respectively, it is shown that the efficiency of cycle depends on pressures of feed water heaters. Pressures of feed water heaters are determined using iterative procedure. Volume flow rate in low-pressure turbine and size of low-pressure turbine are found to be much less in ammonia-water binary-vapour cycle than while using steam only. Mathematical functions for some thermodynamic properties have been developed using least square interpolations. Energy used for evacuation in condenser and evacuation system are trivially eliminated in this cycle. Size of the low-pressure turbines and condenser are reduced significantly compared to existing systems. Diameter of low-pressure turbine in binary-vapour cycle is 20%, 8% at the inlet and exit respectively than while using steam only at 165.4 bar boiler pressure.

Contents

List of Figures

List of Tables

Nomenclature

A	Area (m^2)
c	Thickness coefficient
D	Diameter (m)
h	Enthalpy (kJ/kg)
h_f	Enthalpy of saturated liquid (kJ/kg)
h_g	Enthalpy of saturated vapour (kJ/kg)
l	Nozzle height (m)
$\dot{m}$	Mass flow rate (kg/sec)
p	Pressure (bar)
p_s	Saturation pressure (bar)
p_c	Critical pressure (bar)
$\dot{Q}$	Volume flow rate (m^3/sec)
q_c	Critical liquid density (kg/m^3)
q_l	Density of saturated liquid (kg/m^3)
R	Gas constant (kJ/kg K)
s	Entropy (kJ/kg k)
s_f	Entropy of saturated liquid (kJ/kg k)
s_g	Entropy of saturated vapour (kJ/kg k)
T	Temperature (K)
T_c	Critical temperature (K)
t_s	Saturation temperature (K)
v	Specific volume (m^3/kg)
v_f	Specific volume of saturated liquid(m^3/kg)
v_g	Specific volume of saturated vapour (m^3/kg)

v_c	Critical specific volūme (m^3/kg)
V	Velocity (m/sec)
W_{net}	Net work (kW)
Wp	Work input to pump (kW)
W_t	Work output of turbine (kW)
α	Nozzle angle
η_c	Efficiency of the cycle
η_{HE}	Efficiency of the heat exchanger
η_p	Pump efficiency
η_t	Turbine efficiency
ρ	Density (kg/m^3)

Chapter 1

Introduction

1.1 Description

The ideal power cycle is a Carnot cycle for which the thermal efficiency of heat engine depends on the temperatures T_1 and T_2 of source and sink, respectively.

$$\eta_c = 1 - \frac{T_2}{T_1} \tag{1.1}$$

The processes involved in Carnot cycle are:

- Reversible adiabatic compression
- Reversible heat addition (isothermal process) at T_1
- Reversible adiabatic expansion
- Reversible heat rejection (isothermal process) at T_2

It is not possible to have actual power cycle working on Carnot principle. The phase change cycle (Rankine cycle) approaches the processes of Carnot cycle, i.e., reversible heat addition and reversible heat rejection take place as they occur by phase change processes. Expansion is also reversible adiabatic.

However, for fuel cells the thermal efficiency is not limited by Carnot value. It may have the efficiency of energy conversion far in excess of Carnot efficiency [4].

Only heat addition during sensible heating is not reversible. The working fluid predominately used in phase change cycle is water. It has most of the desirable properties for the use in thermal power cycle as is evident from the following brief description.

1. The *latent heat of vaporization* should be as large as possible and *specific heat* low so that relatively little heat is required to raise the liquid temperature to its boiling point.

2. The *critical temperature* should be well above the metallurgical limit so that reversible heat transfer occurs at constant temperature during phase change of the working fluid at the high temperature of cycle.

3. At the highest operating temperature the pressure should be moderate.

4. The con*denser pressure* should be positive so that there is neither leakage of air into the system nor need for use of the evacuation system.

5. *Saturated vapour line* should lie very close to the path of steam expansion to keep the moisture content at the end of expansion within allowed limit of 10% to 12%.

6. *Specific volume* should be low so that volume flow rate in the turbine is low. Thus, the turbine size becomes small.

7. The *freezing point* should be far below the condensing temperature.

8. It should be *non-flammable, non-poisonous, non toxic,* etc.

9. It should be available in *abundance at low cost.*

Steam satisfies most of the requirements. However, deficiencies with regard to the properties of steam are, negative condensing pressure (0.07384 bar at 313 K), abnormally high boiler pressure (150.0 bar) and tremendously large specific volume (19.54 m^3/kg at 313 K).

1.2 Binary-Vapour Cycle

A typical binary-vapour cycle is shown in figure 1.1. It has high boiling fluid steam in the *topping cycle* and low boiling fluid ammonia in the *bottoming cycle.* The condenser of the topping cycle transfers heat for boiling of working substance of the bottoming cycle to render vapour for the same. The binary-vapour power cycle renders improved thermal efficiency due to use of two fluids. Water-mercury binary-vapour cycle was tried long back [10]. The ammonia-water binary-vapour cycle is a suitable choice to overcome the problems regarding properties mentioned at serial numbers 4, 5, 6 in sec. 1.1.

Despite toxic nature of ammonia, its use has been accepted due to its zero ODP (Ozone depleting potential) and zero GWP (Global warming potential). Ammonia has positive condenser pressure (15.55 bar at 313 K), and very low specific volume (0.0833 m^3/kg at 313 K). At 313 K ammonia has 1/250 and at 293 K 1/400 specific volume of steam. So steam must be expanded to atmospheric pressure only. Ammonia, as its critical temperature (405.5 K) is low, replaces low-pressure steam turbines for bottoming cycle only. Steam is used in the topping cycle in the ammonia-water binary-vapour cycle. Condenser of topping cycle acts as thermal reservoir for boiling of ammonia of the bottoming cycle. Problem of air leakage into the condenser for ammonia-water binary cycle is eliminated due to positive condenser pressure of ammonia. A

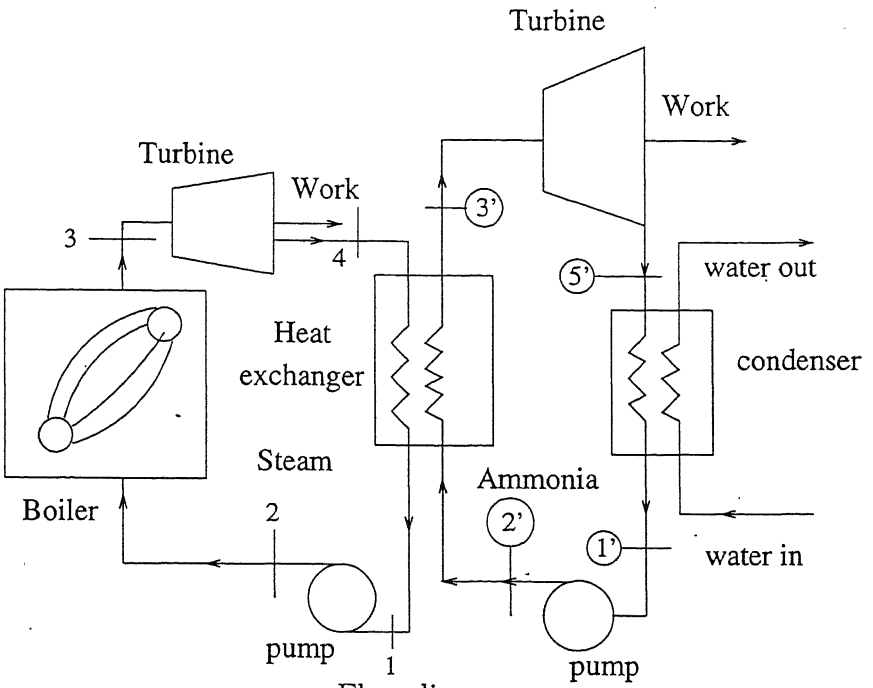

a. Flow diagram

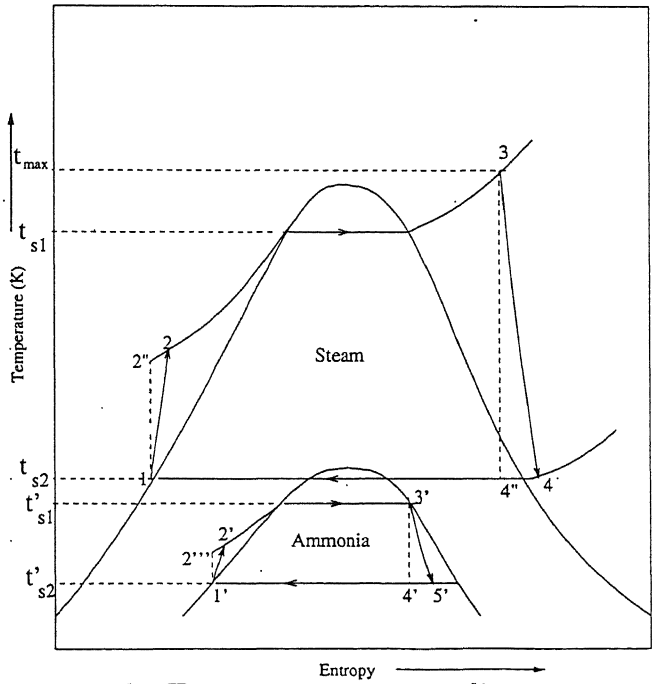

b. Temperature-entropy diagram

Figure 1.1: Ammonia-water binary-vapour system

continuous evacuation system is trivially eliminated. Further the turbine size of low-pressure stage becomes quite small because of low specific volume of ammonia. A single-flow ammonia turbine can replace several double-flow low-pressure steam turbines [7].

1.3 Literature Survey

A high initial temperature is necessary in order to attain a high thermal efficiency for conversion of heat to mechanical energy. Steam suffers from the disadvantages that high pressures and superheating are required in order to obtain high temperature. On the other hand, steam is satisfactory for the utilization of low-pressure, but at low-pressure high specific volume of steam leads to abnormally large size steam turbine. It has therefore been proposed to use top fluids with low-vapour pressure at high temperature, steam for medium and moderately low-pressure and bottom fluids with low specific volume [7].

In binary-vapour cycles, working substances like diphenyl oxide, mercury in topping cycle with steam in bottoming cycle have been used.

Diphenyl oxide has a high freezing point. Thus, danger of freezing in pipe line is serious. Diphenyl oxide has a tendency to decompose above 753 K and has a very high vapour pressure above the 753 K temperature.

Mercury has a critical temperature greater than 1823 K and critical pressure greater than 200 bar. However, if mercury expands in a turbine to 383 K saturation temperature, its corresponding pressure is highly negative (0.000625 bar at 383 K), i.e. high vacuum and a tremendous volume of mercury has to be handled. Mercury is poisonous and highly injurious to health and attacks most of the metals in common use. Each kW of installed capacity requires 1.8 kg of mercury and 14 to 18 kg of mercury vapour has to be condensed to

vaporise 1 kg of water vapours. With mercury being very costly, the cost of plant becomes enormously high. Mercury does not wet boiler and condenser surfaces, so it gives poor heat transfer characteristics.[9]

Fluids like ammonia, methyl chloride and ethyl bromide are the working media in the bottoming cycle with steam being used in the topping cycle. Some CFCs (R-11, R-114, R-113) were also used for the bottoming cycle. CFCs are being phased out due to Ozone hole and GWP problems. For the top fluid used in conjunction with water, a eutectic mixture of diphenyl and diphenyl oxide has been proposed. The mercury / benzene binary-vapour cycle, suggested for possible adoption, would eliminate water as a working fluid. The low specific heat of liquid benzene, about 1.7 kJ/kg K should be viewed in the light of a comparatively low value of the energy of evaporation. Liquid metals, particularly potassium and sodium oxide are used in nuclear electric power plants devised for space applications. In a potassium/steam binary-vapour cycle, potassium turbine would be supplied with potassium vapour at about 2 bar and 1103 K. [10]

1.4 Present Work

A computer programme has been developed to analyse the water-ammonia binary-vapour cycle with different number of feed water heaters. Saturation temperatures in feed water heaters are determined in a way to get maximum efficiency of the cycle. Saturation temperature in condenser is taken as 303 K, 313 K. Range of saturation temperature in boiler is from 473 K to 623 K. Calculations have been carried out for 100 MW power plant. Maximum temperature in the cycle is taken as 823 K. Ammonia boiling temperature range is from 363 K to 391 K. Volume flow rate at the inlet of low-pressure

turbine in binary-vapour cycle is much less than while using steam only.

Chapter 2

Binary-Vapour Power System

2.1 Binary-vapour System

Figure 2.1 shows a simple binary-vapour system. In this system two working fluids are selected on the basis of their desirable properties, such that the overall efficiency of the system gets improved compared to steam power plant cycle. In topping cycle steam is used with ammonia in bottoming cycle. Heat rejected in the condensation of steam is used for boiling of ammonia. Water from pump 1 at point 6 enters in the boiler. Heat is added to water, to get superheated steam. At point 7, temperature of steam is 823 K. The superheated steam at state 7 enters the turbine, where it expands to the pressure p_2, expansion process in turbine is not isentropic. After expansion $\dot{m}_1$ mass of steam is extracted for feed water heating in feed water heater FH 1. Remaining mass ($\dot{m}$-$\dot{m}_1$) enters the turbine at state point 9, where it expands to pressure p_3. After expansion $\dot{m}_2$ mass of steam is extracted for feed water heating in feed water heater FH 2, remaining mass ($\dot{m}$-$\dot{m}_1$-$\dot{m}_2$) enters the turbine at state point 11, where it expands to a pressure p_4. At state point 13, steam enters in the heat exchanger of steam and ammonia, where steam is condensed by evaporating ammonia.

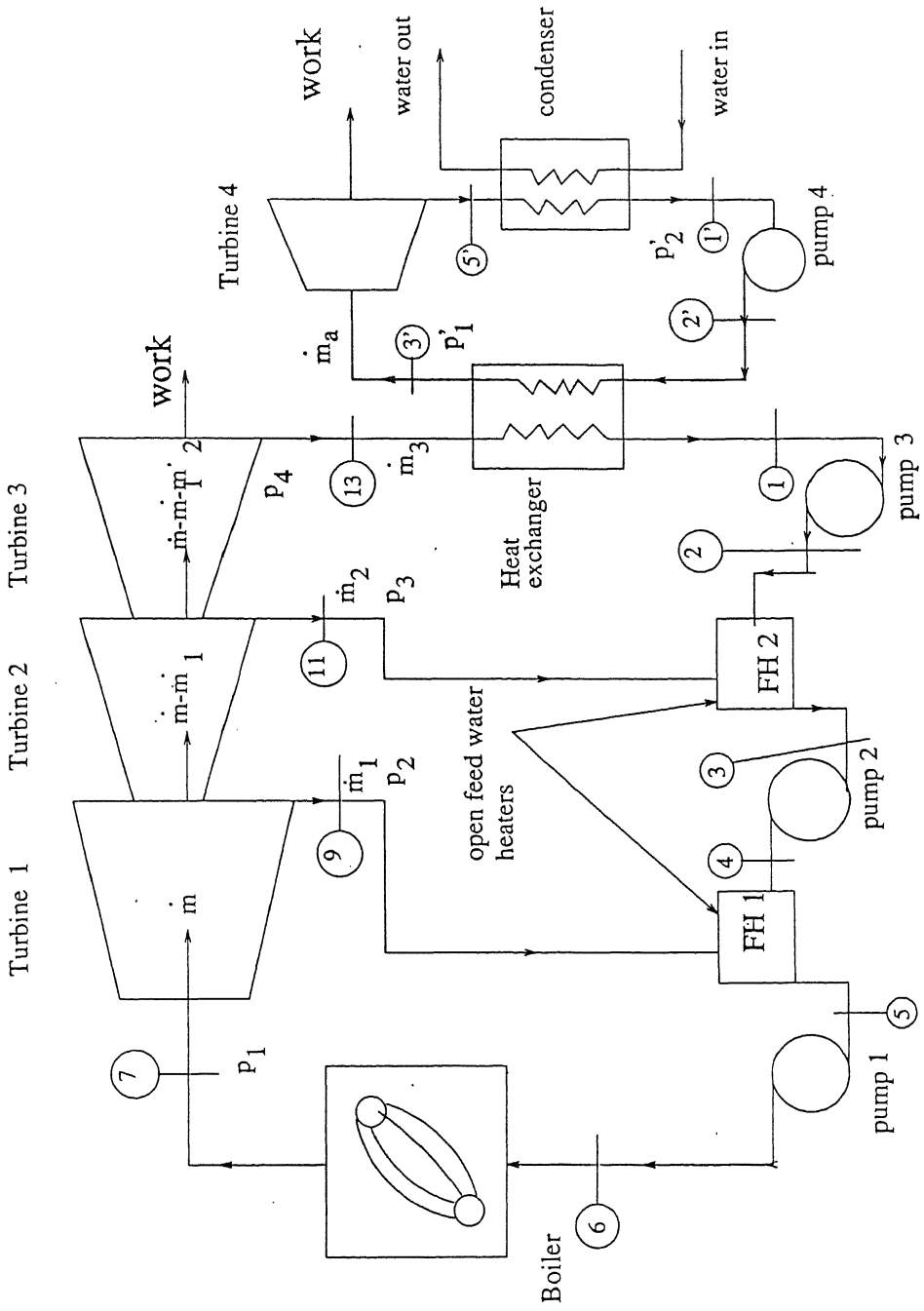

Figure 2.1: Ammonia-water binary-vapour system

Condition of steam at the exit of heat exchanger is saturated liquid. The liquid enters the pump at state point 1 at the condenser pressure p_4. The liquid is raised upto a pressure p_3. This mass $\dot{m}_3$ at pressure p_3 is mixed in feed water heater FH 2 with steam vapour of mass $\dot{m}_2$ extracted at point 11. Condition of steam at the exit of feed water heater is saturated liquid. At point 3, this mass $(\dot{m}_2+\dot{m}_3)$ enters the pump at pressure p_3. The liquid is raised upto a pressure of p_2. This mass $(\dot{m}_2+\dot{m}_3)$ is mixed in feed water heater FH 1 with steam vapours of mass $\dot{m}_1$ extracted at point 9. After mixing condition of steam is saturated liquid. At point 5, this mass $\dot{m}$ enters the pump at pressure p_2, where it is raised upto a pressure p_1.

In the bottoming cycle ammonia enters the heat exchanger at pressure $p_1^{'}$ where it is evaporated by condensing steam. Ammonia is evaporated till it becomes saturated vapour. At state point 3' it enters the turbine, where it expands to pressure $p_2^{'}$ (condenser pressure). Ammonia at point 5' enters the condenser where its latent heat is removed by circulating water. At point 1' ammonia enters the pump at pressure $p_2^{'}$ where its pressure is raised upto pressure $p_1^{'}$. At point 2' ammonia enters the heat exchanger.

2.2 Efficiency of Binary-Vapour Power Cycle

Let η_1 and η_2 be efficiencies of topping cycle and bottoming cycle respectively, then the binary-vapour cycle efficiency (η) is given as [8] :

$$\eta = \eta_1 + \eta_2 - \eta_1\eta_2 \tag{2.1}$$

Equation 2.1 can be written as

$$\eta = \eta_1 + \eta_2(1 - \eta_1) \tag{2.2}$$

$$\eta = \eta_2 + \eta_1(1 - \eta_2) \tag{2.3}$$

$\eta_1 < 1$, $\eta_2 < 1$, so $\eta > \eta_1$, $\eta > \eta_2$

If $\eta_1 = 0.3$, $\eta_2 = 0.3$ then $\eta = 0.51$

So binary-vapour cycle efficiency is higher than cycle using single fluid.

2.3 Operating Conditions

The operating conditions for the present system have been decided based on pressures and temperatures of existing power plants. For ammonia side the upper temperature has been decided based on the positive condensing pressure of low-pressure steam turbine. From this consideration condensation temperature of steam is kept 10 K above the ammonia boiling temperature. Ammonia has a critical temperature of 405.5 K. Saturation pressure of steam is 1.01325 bar at 373 K. So we keep minimum condensation temperature of steam as 373 K to avoid vacuum problem, so minimum boiling temperature of ammonia is (373 K-10 K), i.e., 363 K. We also fix the maximum limit of boiling temperature of ammonia as 391 K well below the critical temperature (405.5 K) of ammonia. Critical temperature of steam is 647 K. Maximum saturation temperature of steam in the boiler is taken as 623 K. At 623 K saturation pressure of steam is 165.4 bar. Steam is superheated upto 823 K. Feed water heater pressures p_2, p_3 are determined in a way to get maximum efficiency of cycle. Condensation temperature of ammonia is taken as 303 K, 313 K. At 313 K saturation pressure of ammonia (15.5 bar) is above the atmospheric pressure. So in ammonia-water

binary-vapour cycle there is no problem of vacuum. Heat exchanger efficiency is taken as 90%. Expansion processes in the turbines are not isentropic, isentropic efficiency of turbine is taken as 86%. Pump efficiency is taken as 75%.

Chapter 3

Mathematical Modelling

3.1 Binary-Vapour Power System

Figure 2.1 shows the schematic diagram of binary-vapour cycle system with two feed water heaters in the topping cycle . This cycle is shown on T-s digram in figure 3.1 .

$\dot{m}$=mass flow rate in the boiler (kg/sec)

$\dot{m}_1$=mass flow rate in the high pressure feed water FH 1 (kg/sec)

$\dot{m}_2$=mass flow rate of in the low-pressure feed water heater FH 2 (kg/sec)

$\dot{m}_3$=mass flow rate of steam in the heat exchanger (kg/sec)

$\dot{m}_a$=mass flow rate of ammonia (kg/sec)

p_1=boiler pressure (bar)

p_2=saturation pressure in high pressure feed water heater FH 1 (bar)

p_3=saturation pressure in low-pressure feed water heater FH 2 (bar)

p_4=steam condensing pressure (bar)

$p_1^{'}$=ammonia boiling pressure (bar)

$p_2^{'}$=condenser pressure (bar)

t_7 =temperature at the exit of boiler=823 K

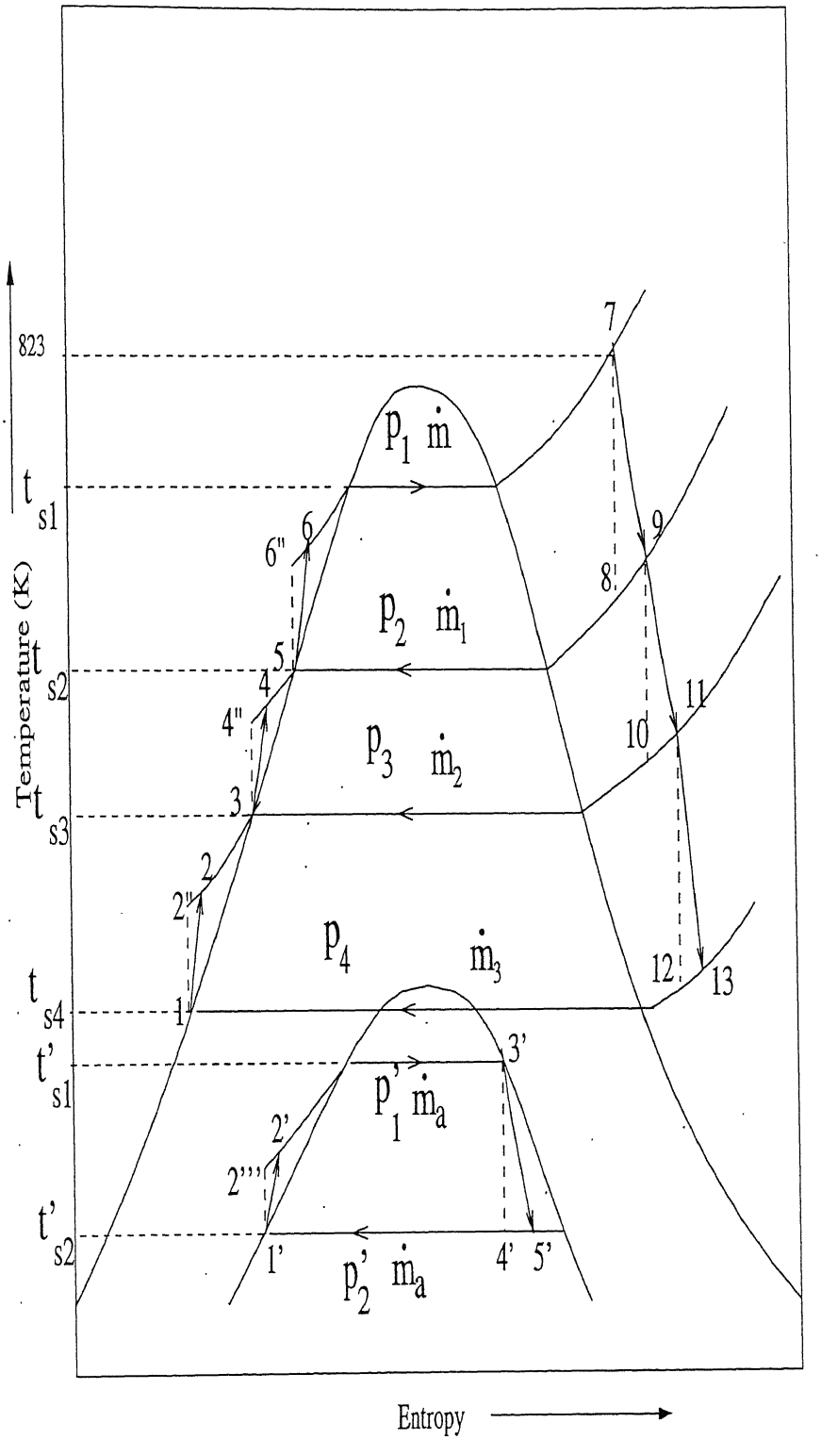

Figure 3.1: Ammonia-water binary-vapour power cycle

t_{s1}, t_{s2}, t_{s3}, t_{s4} are saturation temperature of the steam at the pressure p_1, p_2, p_3, p_4 respectively. t'_{s1}, t'_{s2} are saturation temperature of ammonia at the pressures p'_1, p'_2 respectively. Expansion processes in the turbine (7-9, 9-11, 11-13, $3' - 4'$) are not isentropic. Range of p_1 is from 15 bar to 165.4 bar. A temperature difference of 10 K is maintained between steam condensing temperature and ammonia boiling temperature. Condition of ammonia at point $3'$ is saturated vapour.

η_{HE}=efficiency of the heat exchanger between steam and ammonia=0.90

η_t=isentropic efficiency of the turbine =0.86

η_p=isentropic efficiency of the pump=0.75

t'_{s1}=363 K, 373 K, 383 K, 391 K

t'_{s2}=303 K, 313 K

$$t_{s4} = t'_{s1} + 10 \tag{3.1}$$

$$h_{2''} = h_1 + v_1(p_3 - p_4) \tag{3.2}$$

$$h_2 = h_1 + \frac{(h_{2''} - h_1)}{\eta_p} \tag{3.3}$$

$$h_{4''} = h_3 + v_3(p_2 - p_3) \tag{3.4}$$

$$h_4 = h_3 + \frac{(h_{4''} - h_3)}{\eta_p} \tag{3.5}$$

$$h_{6''} = h_5 + v_5(p_1 - p_2) \tag{3.6}$$

$$h_6 = h_5 + \frac{(h_{6''} - h_5)}{\eta_p} \tag{3.7}$$

$$s_8 = s_7 \tag{3.8}$$

$$h_9 = h_7 - \eta_t(h_7 - h_8) \tag{3.9}$$

$$s_{10} = s_9 \tag{3.10}$$

$$h_{11} = h_9 - \eta_t(h_9 - h_{10}) \tag{3.11}$$

$$s_{12} = s_{11} \tag{3.12}$$

$$h_{13} = h_{11} - \eta_t(h_{11} - h_{12}) \tag{3.13}$$

$$h_{2'''} = h_{1'} + v_{1'}(p_1^{'} - p_2^{'}) \tag{3.14}$$

$$h_{2'} = h_{1'} + \frac{(h_{2'''} - h_{1'})}{\eta_p} \tag{3.15}$$

$$s_{4'} = s_{3'} \tag{3.16}$$

$$h_{5'} = h_{3'} - \eta_t(h_{3'} - h_{4'}) \tag{3.17}$$

Heat rejected in the condensation of the steam is used for boiling of ammonia.

Assume $\dot{m}_3$=1 kg/sec

$$Heat\ taken\ by\ ammonia = Heat\ rejected\ by\ steam \tag{3.18}$$

$$\dot{m}_a(h_{3'} - h_{2'}) = \eta_{HE}\dot{m}_3(h_{13} - h_1) \tag{3.19}$$

$$\dot{m}_a = \frac{\eta_{HE}\dot{m}_3(h_{13} - h_1)}{(h_{3'} - h_{2'})} \tag{3.20}$$

$$\dot{m}_a = \frac{\eta_{HE}(h_{13} - h_1)}{(h_{3'} - h_{2'})} \tag{3.21}$$

$$\dot{m}_2(h_{11} - h_3) = \dot{m}_3(h_3 - h_2) \tag{3.22}$$

$$\dot{m}_2 = \frac{\dot{m}_3(h_3 - h_2)}{(h_{11} - h_3)} \tag{3.23}$$

$$\dot{m}_2 = \frac{(h_3 - h_2)}{(h_{11} - h_3)} \tag{3.24}$$

$$\dot{m}_1(h_9 - h_5) = (\dot{m}_2 + \dot{m}_3)(h_5 - h_4) \tag{3.25}$$

$$\dot{m}_1 = \frac{(\dot{m}_2 + \dot{m}_3)(h_5 - h_4)}{(h_9 - h_5)} \tag{3.26}$$

$$\dot{m_1} = \frac{(\dot{m_2}+1)(h_5 - h_4)}{(h_9 - h_5)} \tag{3.27}$$

From equation 3.24, $\dot{m}_2$ is known so $\dot{m}_1$ is known.

$$\dot{m} = \dot{m}_1 + \dot{m}_2 + \dot{m}_3 \tag{3.28}$$

$$\dot{m} = \dot{m}_1 + \dot{m}_2 + 1 \tag{3.29}$$

From equation 3.24, 3.27 $\dot{m}_2$, $\dot{m}_1$ are known so $\dot{m}$ is known. We have calculated mass flow rate at each point of the system.

$$W_t = \dot{m}(h_7 - h_9) + (\dot{m}_2 + \dot{m}_3)(h_9 - h_{11}) + \dot{m}_3(h_{11} - h_{13}) + \dot{m}_a(h_{3'} - h_{5'}) \tag{3.30}$$

$$W_t = \dot{m}(h_7 - h_9) + (\dot{m}_2 + 1)(h_9 - h_{11}) + (h_{11} - h_{13}) + \dot{m}_a(h_{3'} - h_{5'}) \tag{3.31}$$

$$W_p = \dot{m}_3 v_1(p_3 - p_4) + (\dot{m}_2 + \dot{m}_3)v_3(p_2 - p_3) + \dot{m}v_5(p_1 - p_2) + \dot{m}_a v_{1'}(p_1^{'} - p_2^{'}) \tag{3.32}$$

$$W_p = v_1(p_3 - p_4) + (\dot{m}_2 + 1)v_3(p_2 - p_3) + \dot{m}v_5(p_1 - p_2) + \dot{m}_a v_{1'}(p_1^{'} - p_2^{'}) \tag{3.33}$$

$$W_{net} = W_t - W_p \tag{3.34}$$

$$heat\,added = \dot{m}(h_7 - h_6) \tag{3.35}$$

$$efficiency\,of\,cycle = \frac{net\,work}{heat\,added} \tag{3.36}$$

$$\eta_c = \frac{W_{net}}{\dot{m}(h_7 - h_6)} \tag{3.37}$$

W_{net} is power output for $\dot{m}_3$ =1 kg/sec. We assume the capacity of power plant as 100 MW. For 100 MW power output we have to calculate the mass flow rate at each point of the system.

$$\dot{m}_3 = \frac{100\,MW}{W_{net}} \tag{3.38}$$

From equation 3.20, 3.23, 3.26, 3.28 $\dot{m}_a$, $\dot{m}_2$, $\dot{m}_1$, $\dot{m}$ is known for 100 MW power output.

$$volume\,flow\,rate = specific\,volume * mass\,flow\,rate \tag{3.39}$$

FriFrom equation 3.39 we can calculate the volume flow rate at the inlet and exit of all the turbines.

Saturation temperature in boiler is varied in the range of 473 K to 623 K at the interval of 10 K. Condenser temperature t'_{s2} is kept at 303 K , 313 K. Boiling temperature of ammonia t'_{s1} is kept at 363 K, 373 K, 383 K, 391 K. Range of saturation temperature in the high pressure feed water heater (t_{s2}) and low-pressure feed water heater (t_{s3}) is from t_{s4} to t_{s1} . First we keep t_{s3} 5 K above the t_{s4} and vary t_{s2} in the range of $(t_{s3}+5)$ to $(t_{s1}-5)$ till the efficiency becomes the maximum. Then again increase t_{s3} by 5 K and vary t_{s2} in the range of $(t_{s3}+5)$ to $(t_{s1}-5)$ till the efficiency becomes the maximum. We increase t_{s3} till $(t_{s1}-t_{s3})$ is greater than 10 K and vary t_{s2} in the range of $(t_{s3}+5)$ to $(t_{s1}-5)$ at an interval of 10 K. In this way we can find saturation temperatures in the feed water heaters for maximum efficiency. Thermodynamic properties of ammonia and steam are given in the appendix. A computer program has been developed to analyse the cycle and calculate the maximum efficiency, mass flow rate and volume flow rate at the different points.

3.2 Steam Power System

Figure 3.2 shows the schematic diagram of steam power cycle system with three feed water heaters. This cycle is shown on T-s digram in figure 3.3.

$\dot{m}$=mass flow rate in the boiler (kg/sec)

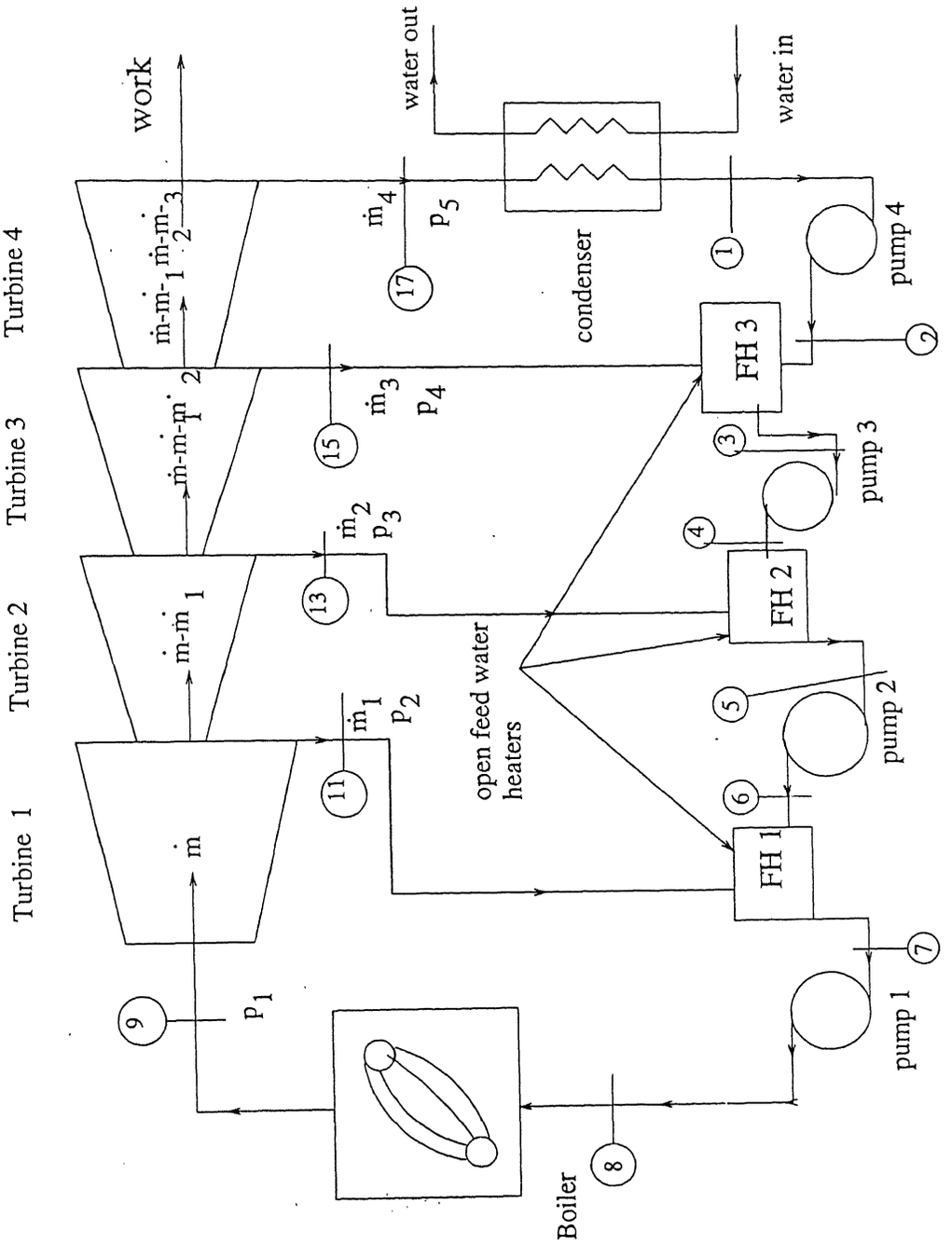

Figure 3.2: Steam power system

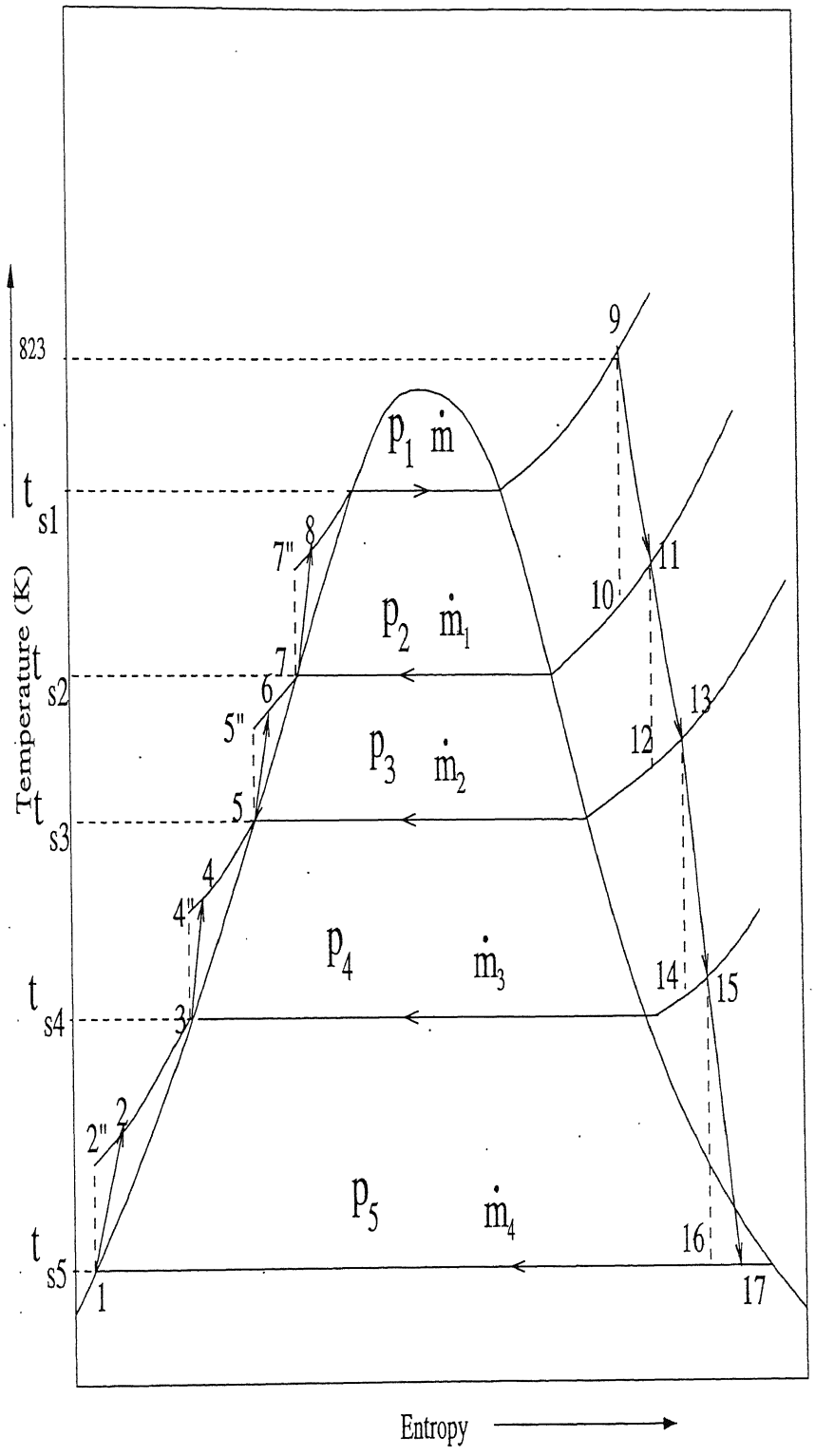

Figure 3.3: Steam power cycle

$\dot{m}_1$=mass flow rate in feed water heater FH 1 (kg/sec)

$\dot{m}_2$=mass flow rate of in feed water heater FH 2 (kg/sec)

$\dot{m}_3$=mass flow rate of in feed water heater FH 3 (kg/sec)

$\dot{m}_4$=mass flow rate of in the condenser (kg/sec)

p_1=boiler pressure (bar)

p_2=saturation pressure in feed water heater FH 1 (bar)

p_3=saturation pressure in feed water heater FH 2 (bar)

p_4=saturation pressure in feed water heater FH 3 (bar)

p_5=condenser pressure (bar)

t_9 =temperature at the exit of boiler=823 K

t_{s1}, t_{s2}, t_{s3}, t_{s4}, t_{s5} are saturation temperature of the steam at the pressure p_1, p_2, p_3, p_4, p_5 respectively. Expansion process in the turbine (9-11, 11-13, 13-15, 15-17) are not isentropic. Range of p_1 is from 15 bar to 165.4 bar.

η_t=isentropic efficiency of the turbine =0.86

η_p=isentropic efficiency of the pump=0.75

t'_{s2}=303 K, 313 K

Analysis of this cycle can be done similarly as given in sec. 3.1.

Chapter 4

Results and Discussions

4.1 Optimum Saturation Temperature of Feed Water Heater

Figure 4.1 shows the variation in efficiency with saturation temperature of feed water heater keeping condenser and boiler pressure constant for steam cycle with one feed water heater. First efficiency increases and becomes maximum before it decreases again. The maximum efficiency is found to occur at the arithmetic mean of saturation temperatures in boiler and condenser [13].

Variation in efficiency with pressure in feed water heater is shown in figure 4.2 keeping condenser and boiler pressure as constant for a steam cycle with one feed water heater.

4.2 Efficiency

Figure 4.3, 4.4 shows the variation in maximum efficiency with boiler pressure while saturation temperature of condenser is kept constant. Maximum efficiencies for steam cycle with one, two, three feed water heaters and binary cycle

with one, two feed water heaters has been obtained by using iterative procedure as explained in section no. 3.1. Efficiency at 165.4 bar for steam cycle without feed water heater is 0.38, while for steam cycle with three feed water heaters is 0.45. For the binary-vapour cycle efficiency is slightly less compared to steam cycle because there is a temperature difference of 10 K in heat exchanger and heat exchanger efficiency is 0.9. As number of feed water heaters are increased, efficiency increases.

Figure 4.5, 4.6 shows the variation in maximum efficiency of a binary-vapour cycle without feed water heater for a fixed boiling pressure of steam and different boiling temperatures of ammonia. Efficiency reduces as ammonia boiling temperature is increased.

Figure 4.7, 4.8 shows the variation in maximum efficiency of a binary-vapour cycle with one feed water heater for a fixed boiling pressure of steam and different boiling temperatures of ammonia. Efficiency reduces as ammonia boiling temperature is increased.

Figure 4.9, 4.10 shows the variation in maximum efficiency of a binary-vapour cycle with two feed water heaters for a fixed boiling pressure of steam and different boiling temperatures of ammonia. Efficiency reduces as ammonia boiling temperature is increased.

4.3 Mass flow Rate in Condenser

Figure 4.11, 4.12 shows the variation in mass flow rate in condenser with boiling pressure of steam. As number of feed water heaters are increased, condenser mass flow rate reduces.

4.4 Mass flow Rate of Ammonia

Figure 4.13 shows the variation in mass flow rate of ammonia with boiling pressure of steam. As number of feed water heaters are increased, mass flow rate of ammonia reduces. At 165.4 bar boiler pressure and 303 K saturation temperature in condenser, mass flow rate of ammonia is 147 kg/sec for binary-vapour cycle without feed water heater, 123 kg/sec for binary-vapour cycle with two feed water heaters.

Figure 4.14, 4.15 and 4.16 shows the variation in mass flow rate of ammonia with boiling pressure of steam without feed water heater, with one and two feed water heaters respectively at different boiling temperatures of ammonia. Mass flow rate of ammonia decreases as boiling pressure of steam increases. Mass flow rate of ammonia is less for low boiling temperatures of ammonia.

4.5 Mass Flow Rate through Boiler

Figure 4.17, 4.18 shows the variation in mass flow rate in boiler with boiling pressure of steam. For steam cycle without feed water heater and binary-vapour cycle without feed water heater mass flow rate in boiler decreases as boiler pressure increases. Mass flow rate in boiler first decreases, becomes minimum before it increases again for steam cycle with one, two, three feed water heaters and binary-vapour cycle with one, two feed water heaters.

Figure 4.19 shows the variation in mass flow rate in boiler of binary-vapour cycle without feed water heater with boiling pressure of steam. Mass flow rate in boiler increases as ammonia boiling temperature increases.

Figure 4.20, 4.21 shows the variation in mass flow rate in boiler of binary-vapour cycle with boiling pressure of steam with one, two feed water heaters

respectively. Mass flow rate in boiler first decreases, becomes minimum before it increases again.

4.6 Volume Flow Rate of Ammonia

Figure 4.22 shows the variation in volume flow rate of ammonia at the inlet of turbine with boiling pressure of steam. As number of feed water heaters are increased, volume flow rate of ammonia decreases. Figure 4.23, 4.24, 4.25 shows the variation in volume flow rate of ammonia at the inlet of turbine with boiling pressure of steam for binary-vapour cycle without feed water heater, with one and two feed water heaters respectively. As ammonia boiling temperature increases, volume flow rate of ammonia decreases.

4.7 Volume Flow Rate in Low-Pressure Stage

Figure 4.26 shows the variation in volume flow rate at the inlet of low-pressure stage turbine with boiling pressure of steam for steam cycle with one feed water heater and binary-vapour cycle without feed water heater. Volume flow rate decreases as boiling pressure increases. Volume flow rate for steam cycle with one feed water heater is more than binary-vapour cycle without feed water heater.

Figure 4.27 shows the variation in volume flow rate at the inlet of low-pressure stage turbine with boiling pressure of steam for steam cycle with two feed water heaters and binary-vapour cycle with one feed water heater. Volume flow rate decreases as boiling pressure increases. At 165.5 bar boiler pressure volume flow rate for steam cycle with two feed water heaters is $34.17 m^3/sec$ and $2.49 m^3/sec$ for binary-vapour cycle with one feed water heater.

Figure 4.28 shows the variation in volume flow rate at the inlet of low-pressure stage turbine with boiling pressure of steam for steam cycle with three feed water heaters and binary-vapour cycle with two feed water heaters. Volume flow rate decreases as boiling pressure increases. At 165.4 bar boiler pressure volume flow rate for steam cycle with three feed water heaters is $68.96m^3/sec$ and $2.92m^3/sec$ for binary-vapour cycle with two feed water heaters.

4.8 Low-Pressure Turbine Size

At 165.4 bar boiler pressure volume flow rate at the inlet, exit of the low-pressure turbine is $68.96m^3/sec$, $1672m^3/sec$ respectively for steam cycle with three feed water heaters is and $2.92m^3/sec$, $11.56m^3/sec$ respectively for binary-vapour cycle with two feed water heaters. For calculating the size of turbine we assume turbine is of impulse type. [6]

$$A = \pi Dlc \sin \alpha \tag{4.1}$$

Where, A=flow area

α=nozzle angle

l =nozzle height

c=thickness coefficient

D=mean diameter of the turbine blade

$$\dot{Q} = AV \tag{4.2}$$

Where, $\dot{Q}$=volume flow rate

V=flow velocity

We take V=120 m/sec, 150 m/sec at the inlet, exit of the turbine respec-

tively.

$$m = \frac{l}{D} \tag{4.3}$$

we take m=0.18, $\alpha = 20°$, c=0.85

From equation 4.1, 4.2, 4.3 we get D=1.87 m, 8.23 m at the inlet, exit of the low stage turbine for steam cycle with 3 feed water heaters at 165.4 bar boiler pressure and D=0.385 m, 0.685 m at the inlet, exit of the low-pressure turbine for binary-vapour cycle with 2 feed water heaters at 165.4 boiler pressure. Low-pressure turbine size for steam cycle with 3 feed water heaters is 5, 12 times of binary-vapour cycle with 2 feed water heaters.

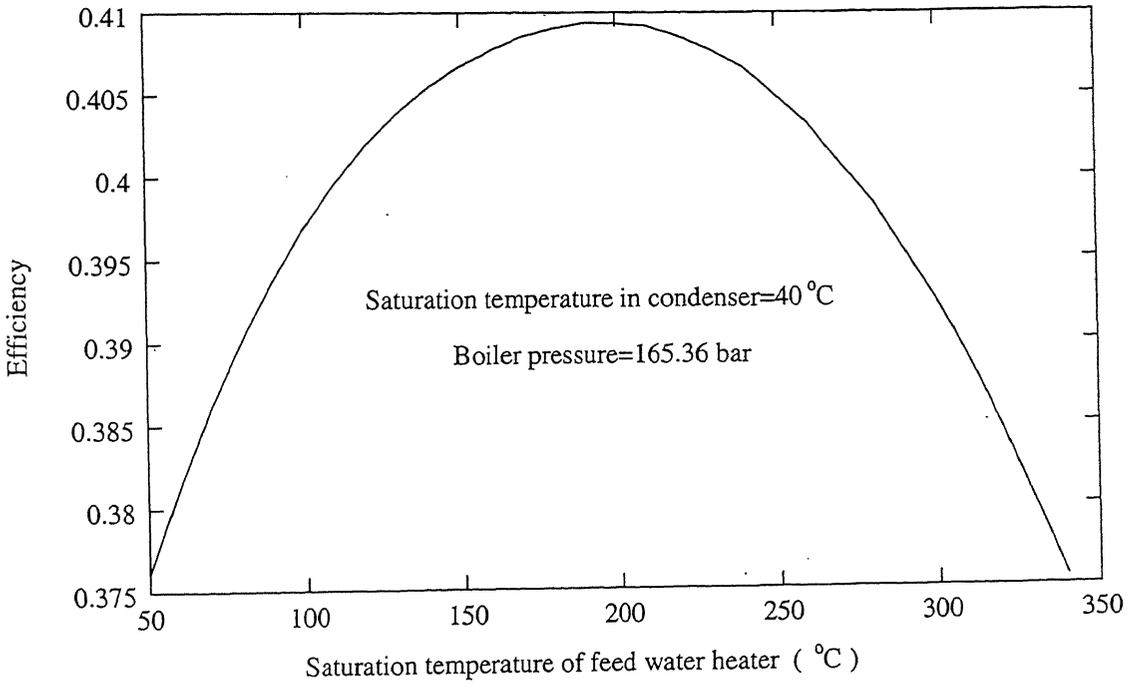

Figure 4.1: Variation in efficiency with saturation temperature of feed water heater of steam cycle with one feed water heater

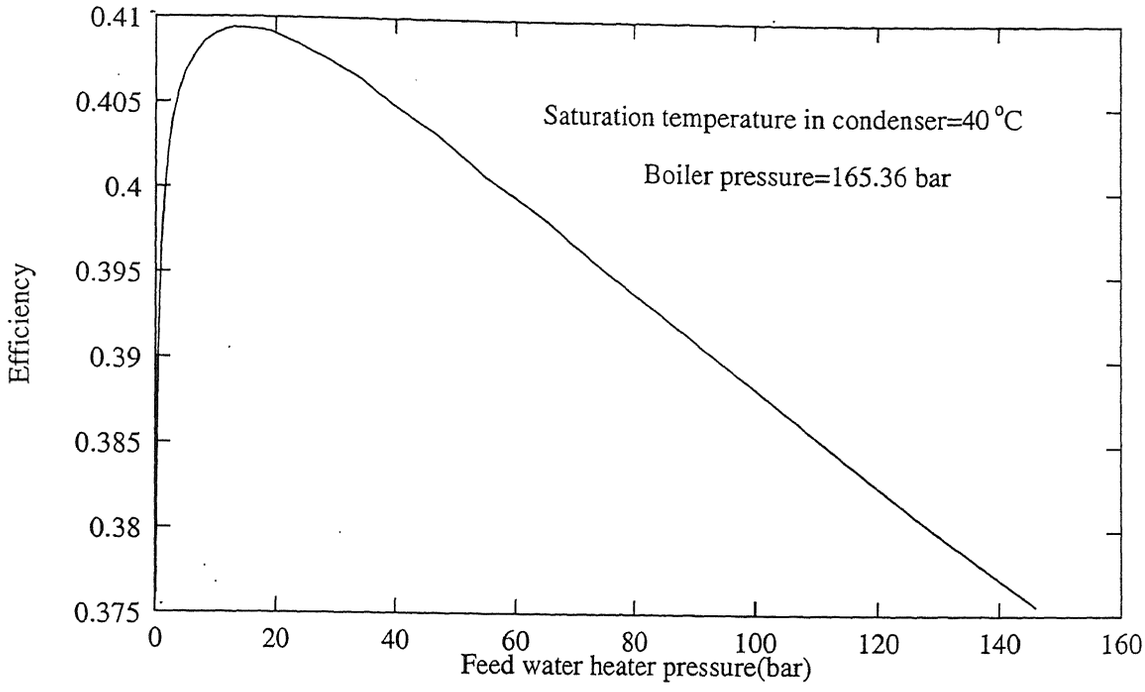

Figure 4.2: Variation in efficiency with feed water heater pressure of steam cycle with one feed water heater

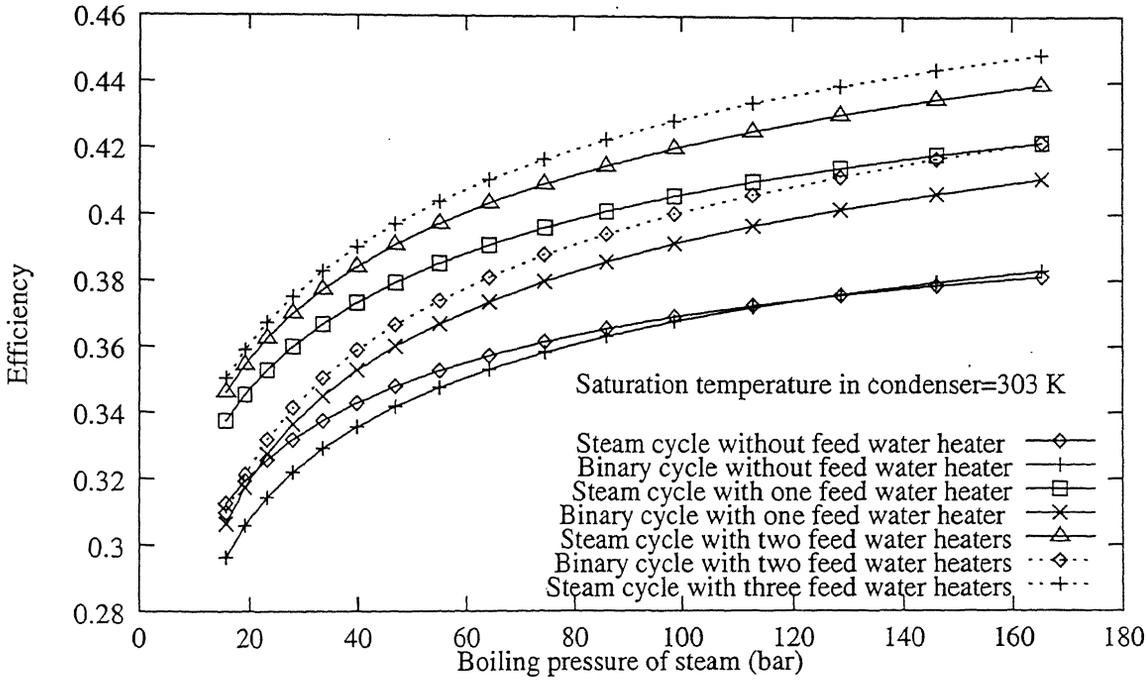

Figure 4.3: Variation in efficiency with boiling pressure of steam at the constant saturation temperature in condenser $=303\,K$

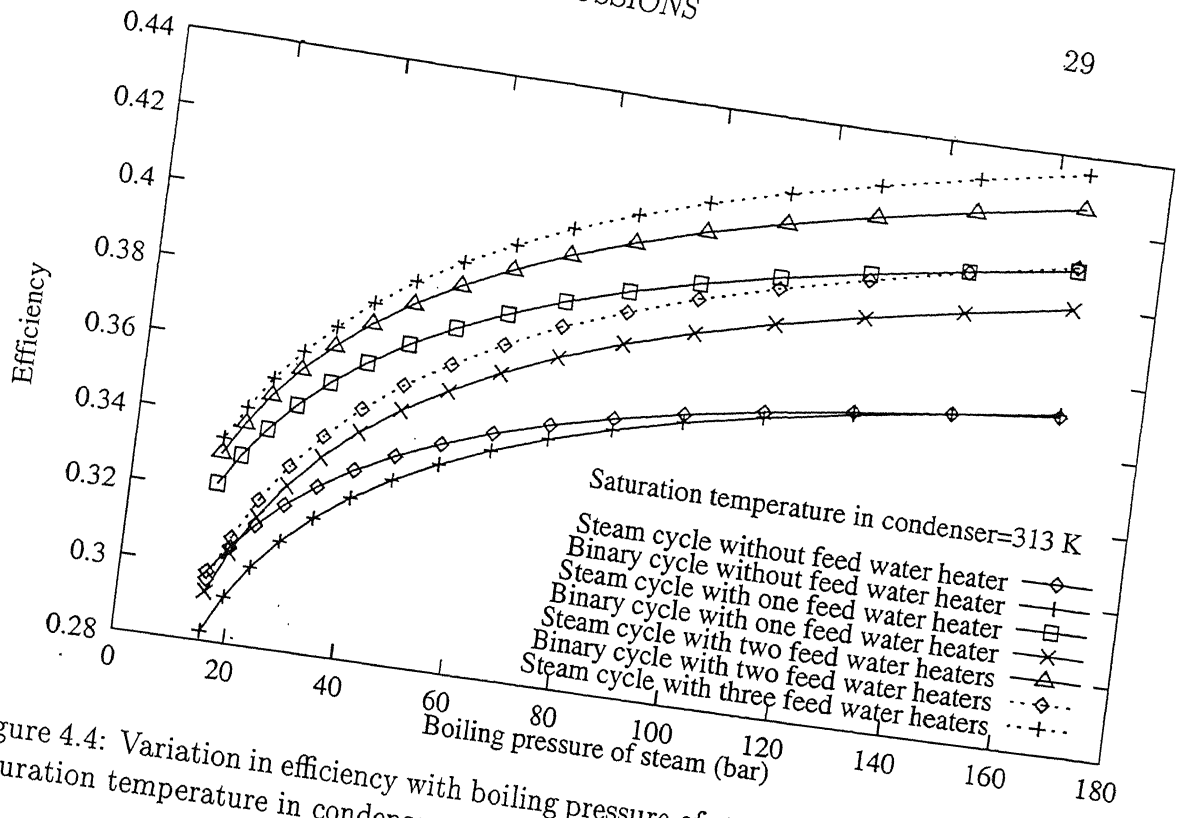

Figure 4.4: Variation in efficiency with boiling pressure of steam at the constant saturation temperature in condenser $=313\,K$

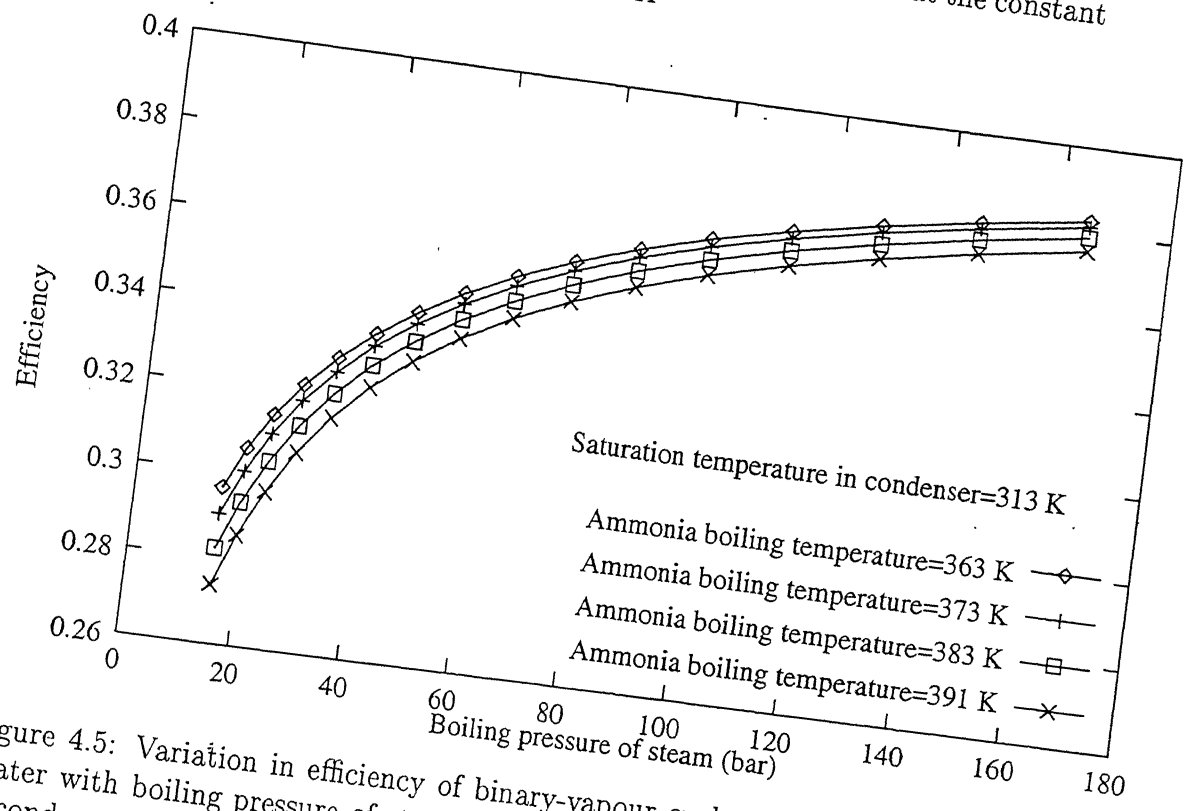

Figure 4.5: Variation in efficiency of binary-vapour cycle without feed water heater with boiling pressure of steam at the constant saturation temperature in condenser $=303\,K$

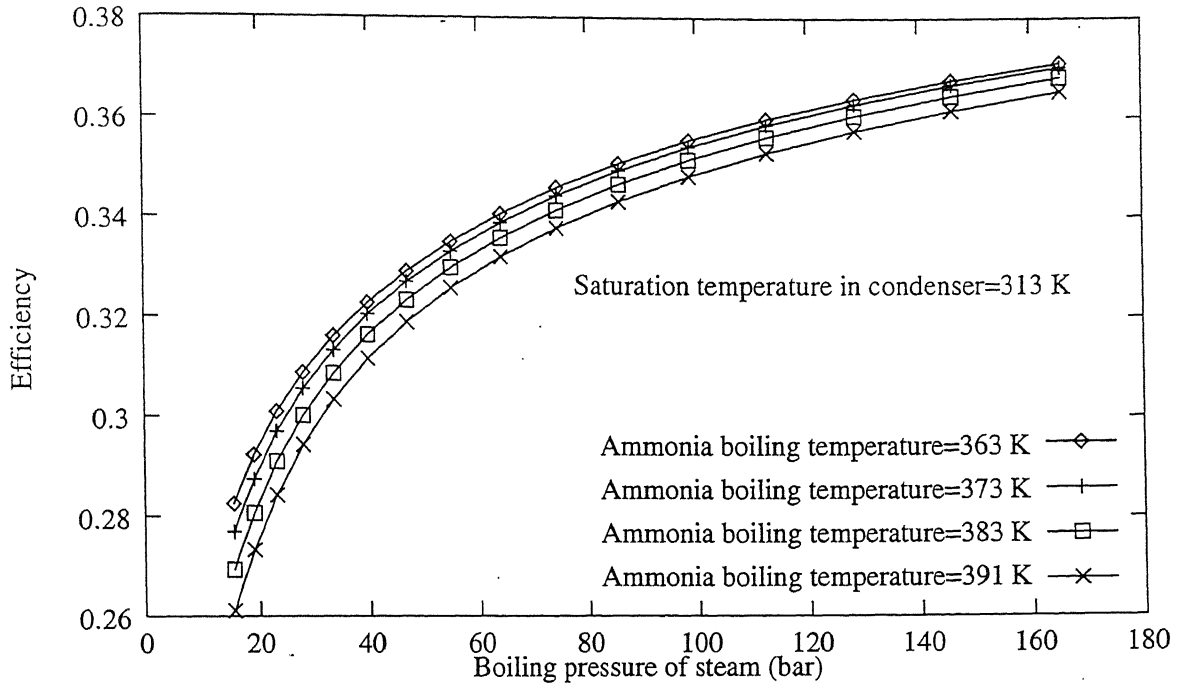

Figure 4.6: Variation in efficiency of binary-vapour cycle without feed water heater with boiling pressure of steam at the constant saturation temperature in condenser $=313\,K$

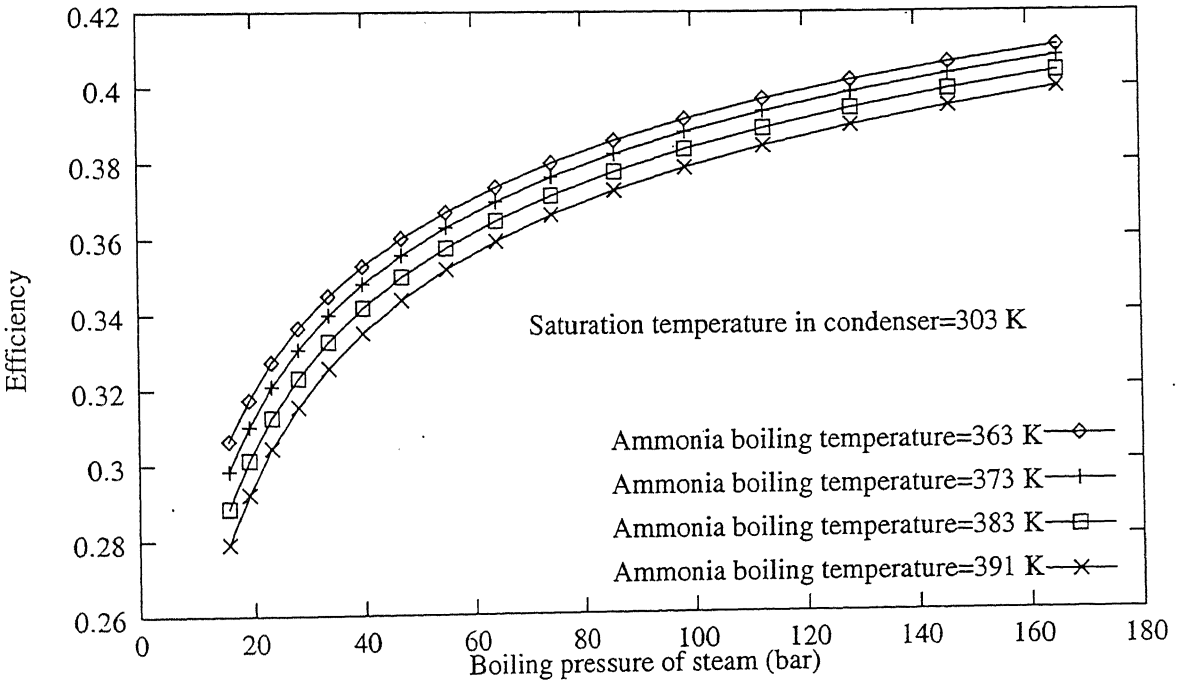

Figure 4.7: Variation in efficiency of binary-vapour cycle with one feed water heater with boiling pressure of steam at the constant saturation temperature in condenser $=303\,K$

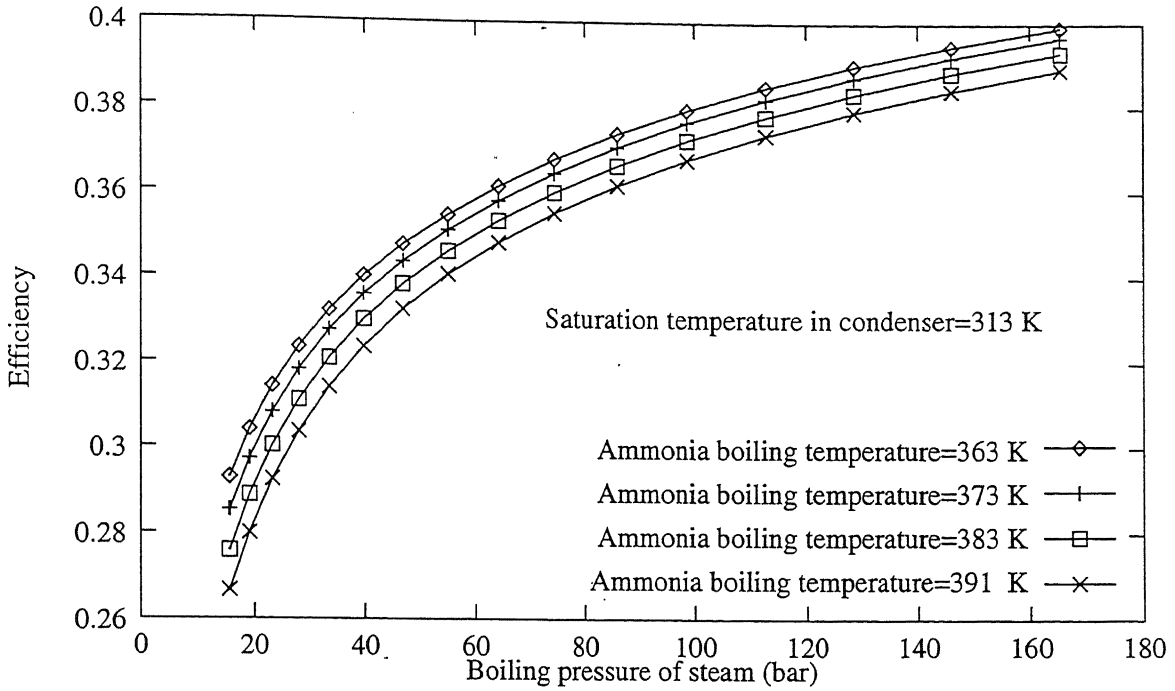

Figure 4.8: Variation in efficiency of binary-vapour cycle with one feed water heater with boiling pressure of steam at the constant saturation temperature in condenser $=313\,K$

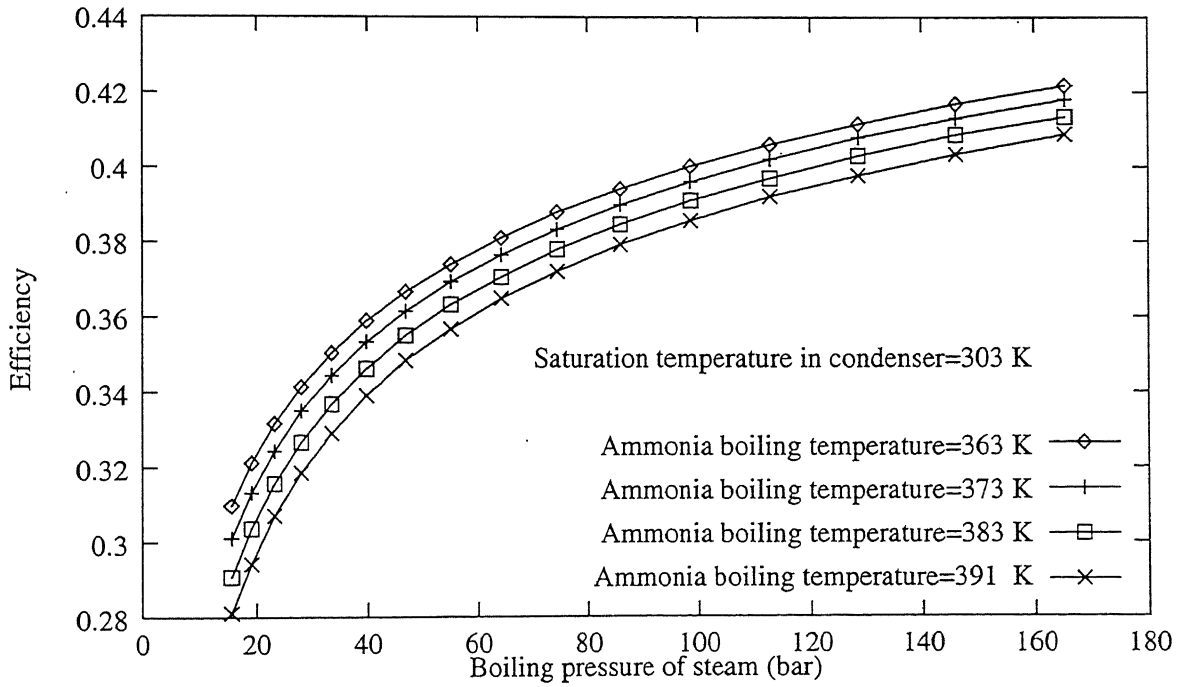

Figure 4.9: Variation in efficiency of binary-vapour cycle with two feed water heaters with boiling pressure of steam at the constant saturation temperature in condenser $=303\,K$

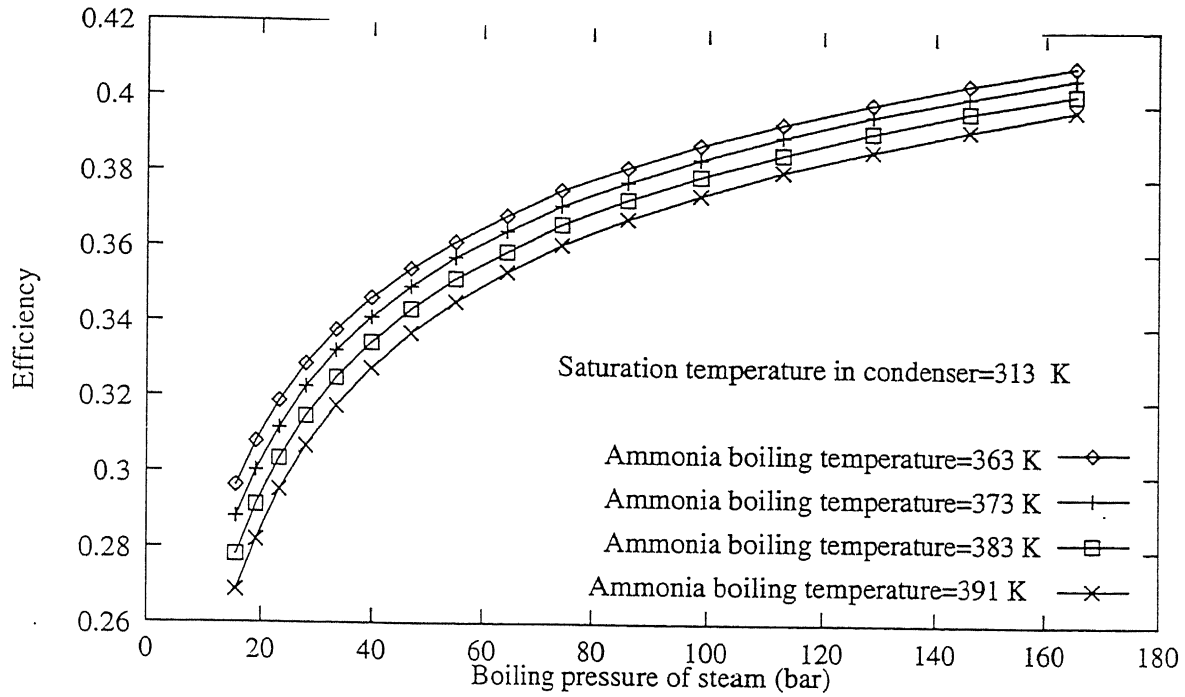

Figure 4.10: Variation in efficiency of binary-vapour cycle with two feed water heaters with boiling pressure of steam at the constant saturation temperature in condenser $=313\,K$

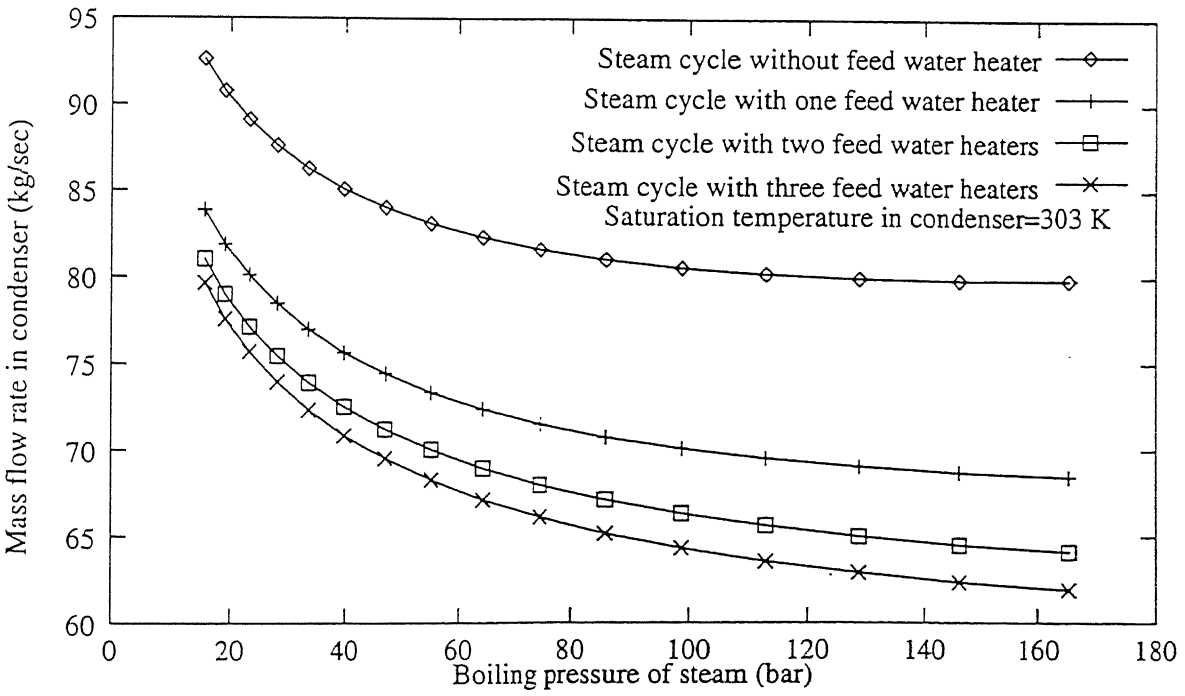

Figure 4.11: Variation in mass flow rate in condenser of steam cycle with boiling pressure of steam at the constant saturation temperature in condenser $=303\,K$

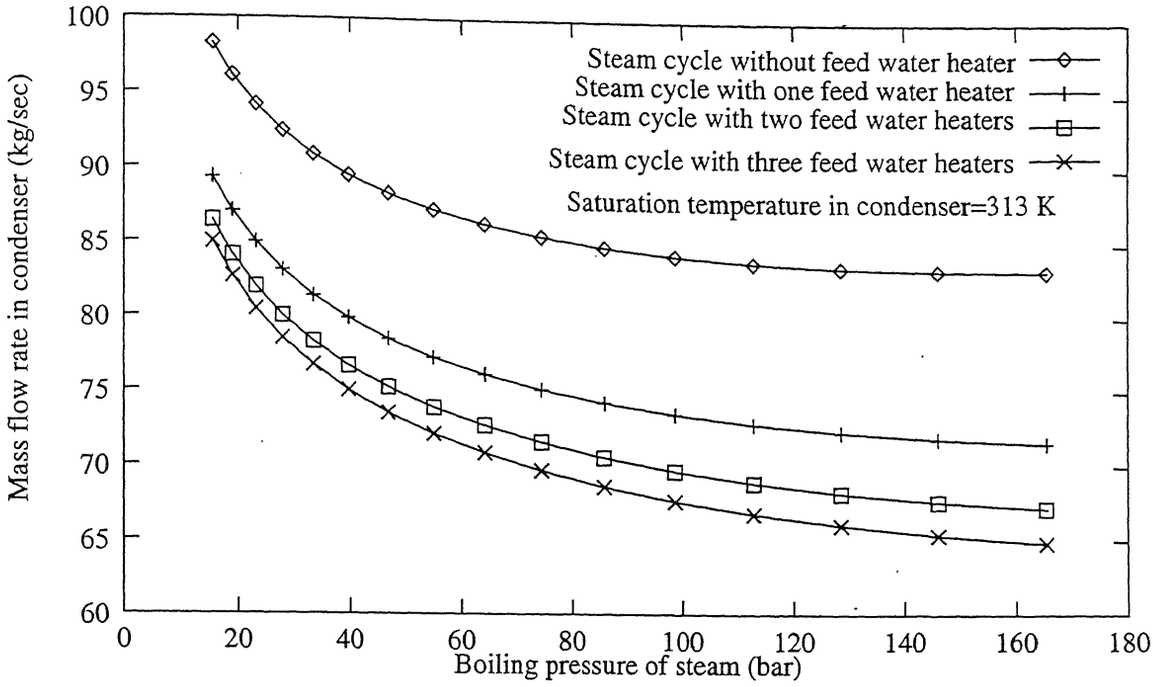

Figure 4.12: Variation in mass flow rate in condenser with boiling pressure of steam at the constant condenser temperature $=313\,K$

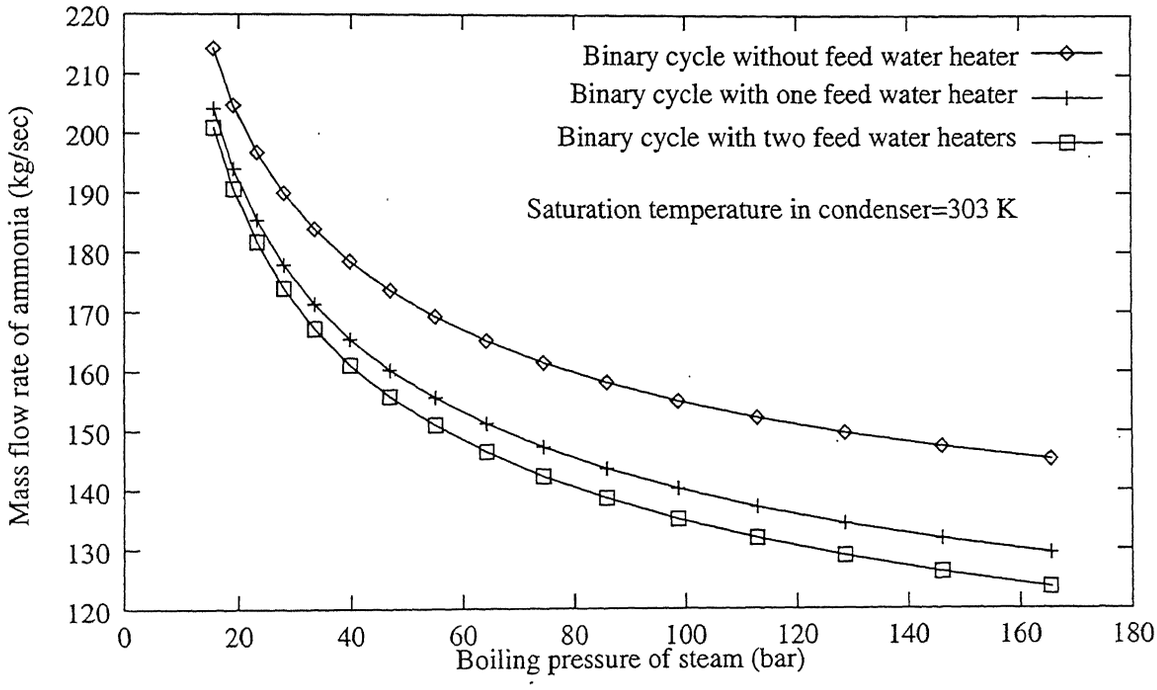

Figure 4.13: Variation in mass flow rate of ammonia of binary-vapour cycle with boiling pressure of steam at the constant saturation temperature in condenser $=303\,K$

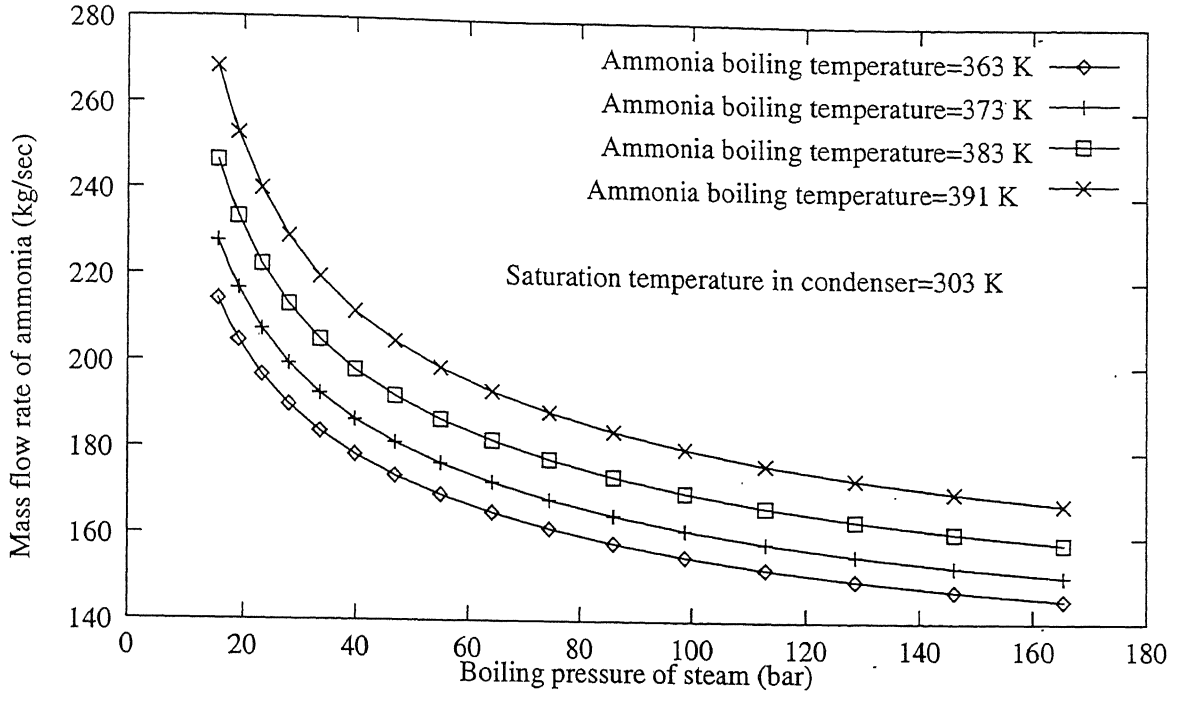

Figure 4.14: Variation in mass flow rate of ammonia of binary-vapour cycle without feed water heater with boiling pressure of steam at the constant saturation temperature in condenser $=303\,K$

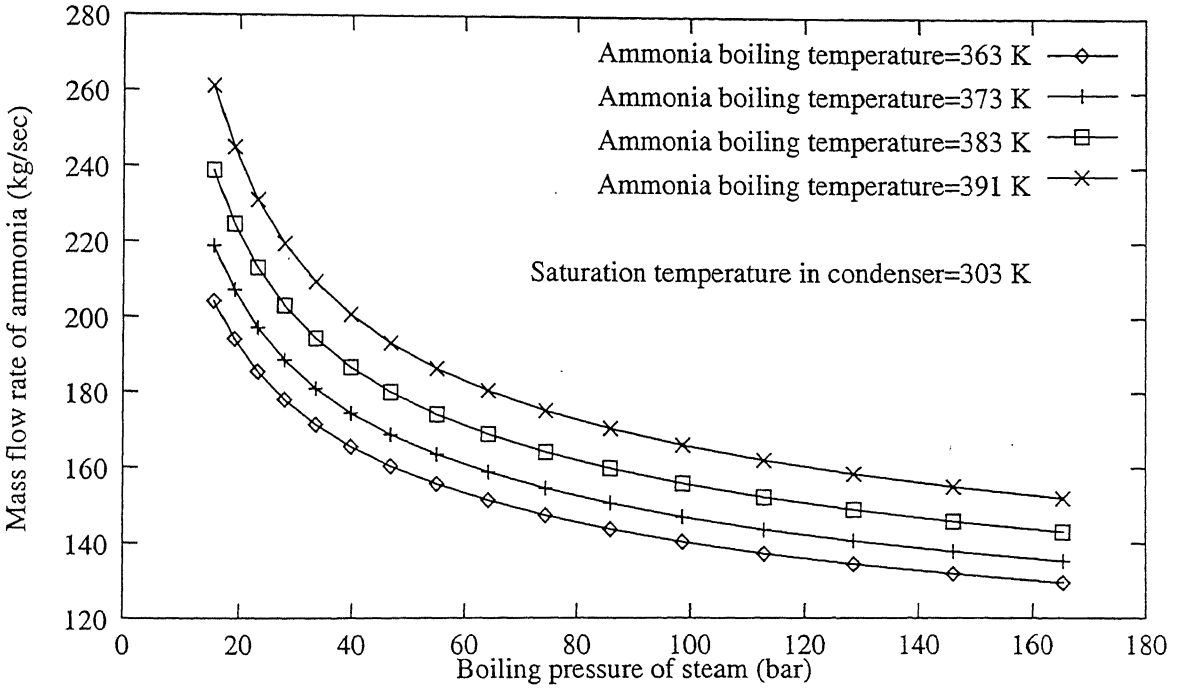

Figure 4.15: Variation in mass flow rate of ammonia of binary-vapour cycle with one feed water heater with boiling pressure of steam at the constant saturation temperature in condenser $=303\,K$

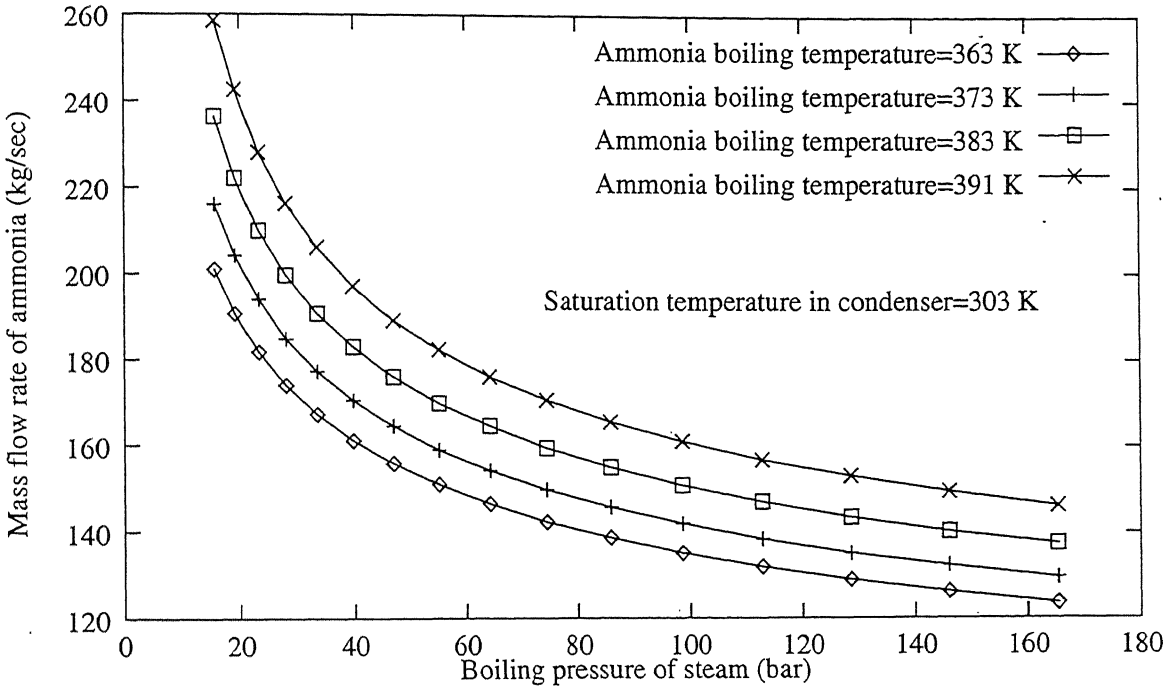

Figure 4.16: Variation in mass flow rate of ammonia of binary-vapour cycle with two feed water heaters with boiling pressure of steam at the constant saturation temperature in condenser $=303\,K$

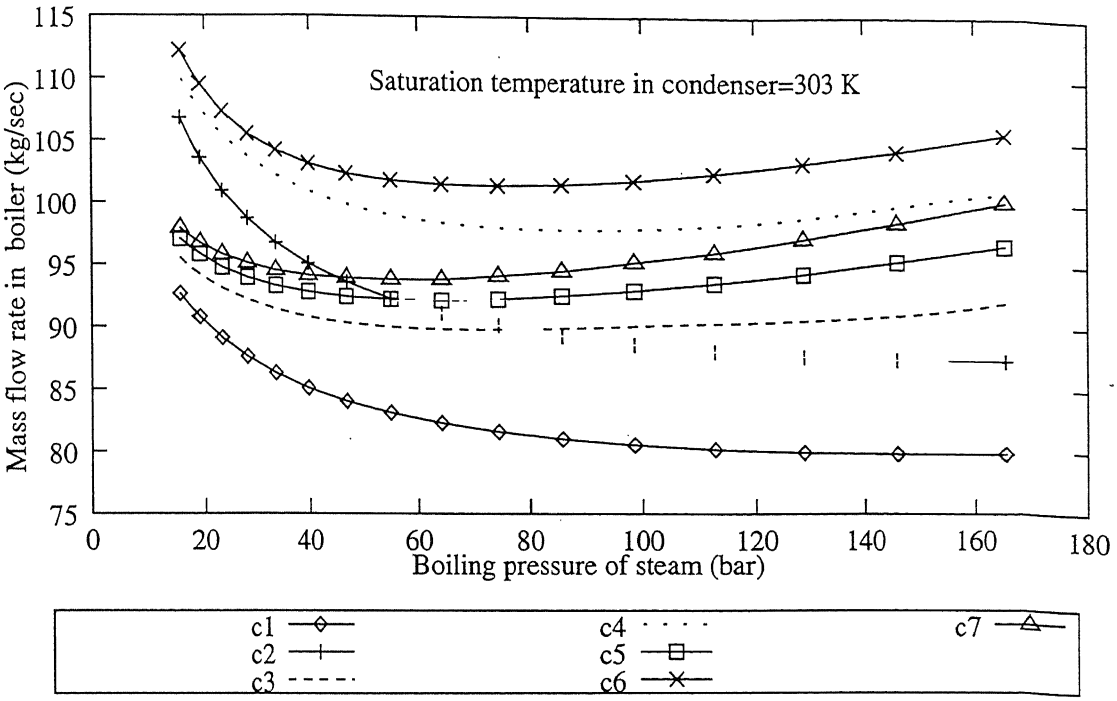

c1 : Steam cycle without feed water heater

c2 : Binary cycle without feed water heater

c3 : Steam cycle with one feed water heater

c4 : Binary cycle with one feed water heater

c5 : Steam cycle with two feed water heaters

c6 : Binary cycle with two feed water heaters

c7: Steam cycle with three feed water heaters

Figure 4.17: Variation in mass flow rate in boiler with boiling pressure of steam at the constant saturation temperature in condenser $=303\,K$

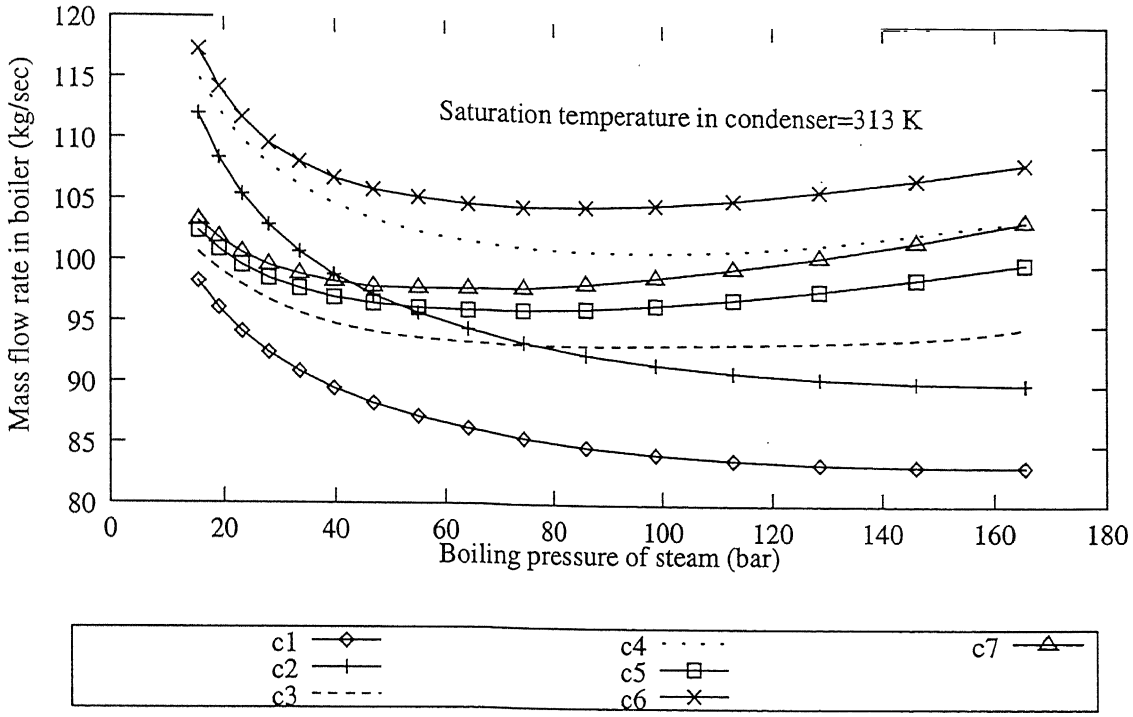

c1 : Steam cycle without feed water heater

c2 : Binary cycle without feed water heater

c3 : Steam cycle with one feed water heater

c4 : Binary cycle with one feed water heater

c5 : Steam cycle with two feed water heaters

c6 : Binary cycle with two feed water heaters

c7: Steam cycle with three feed water heaters

Figure 4.18: Variation in mass flow rate in boiler with boiling pressure of steam at the constant saturation temperature in condenser = $313\,K$

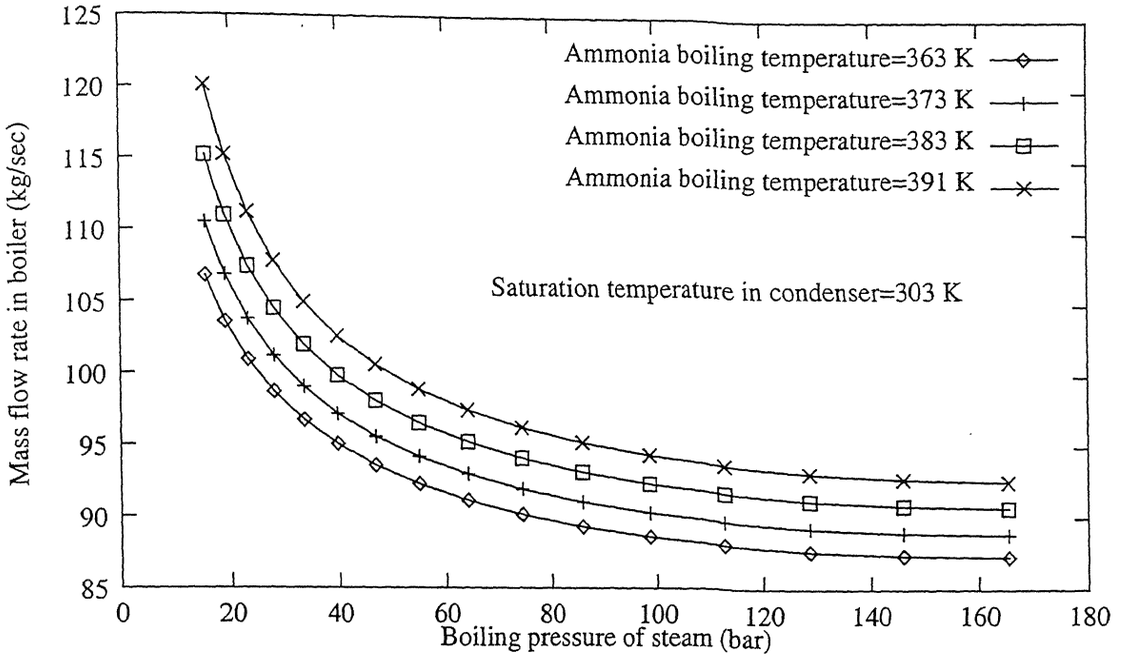

Figure 4.19: Variation in mass flow rate in boiler of binary-vapour cycle without feed water heater with boiling pressure of steam at the constant saturation temperature in condenser $=303\,K$

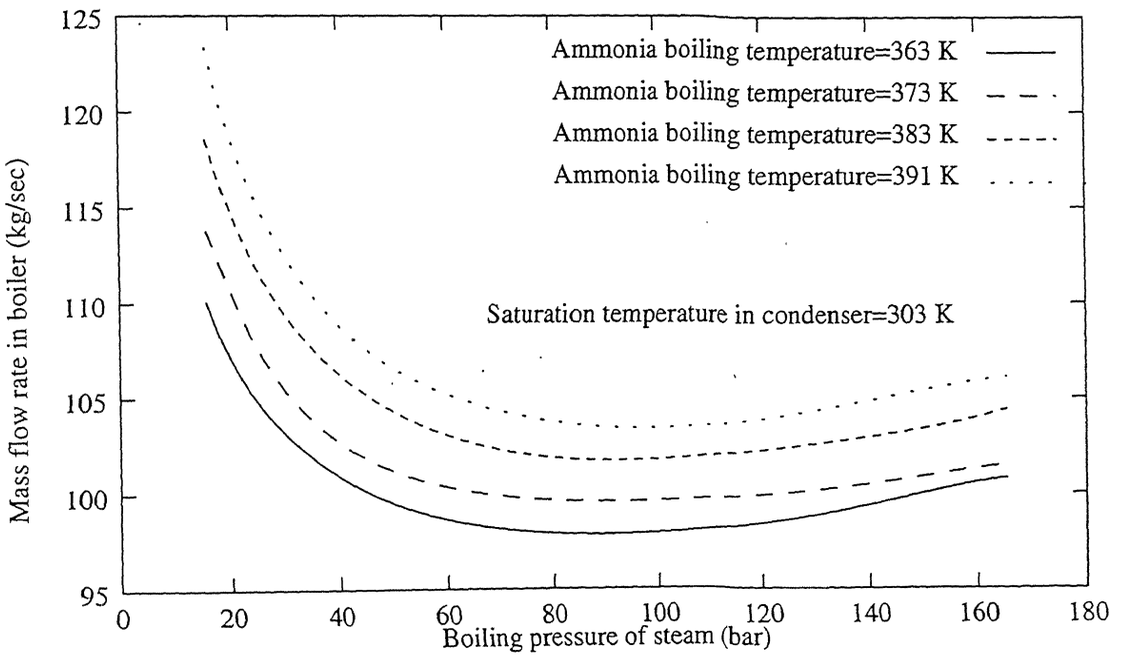

Figure 4.20: Variation in mass flow rate in boiler of binary-vapour cycle with one feed water heater with boiling pressure of steam at the constant saturation temperature in condenser $=303\,K$

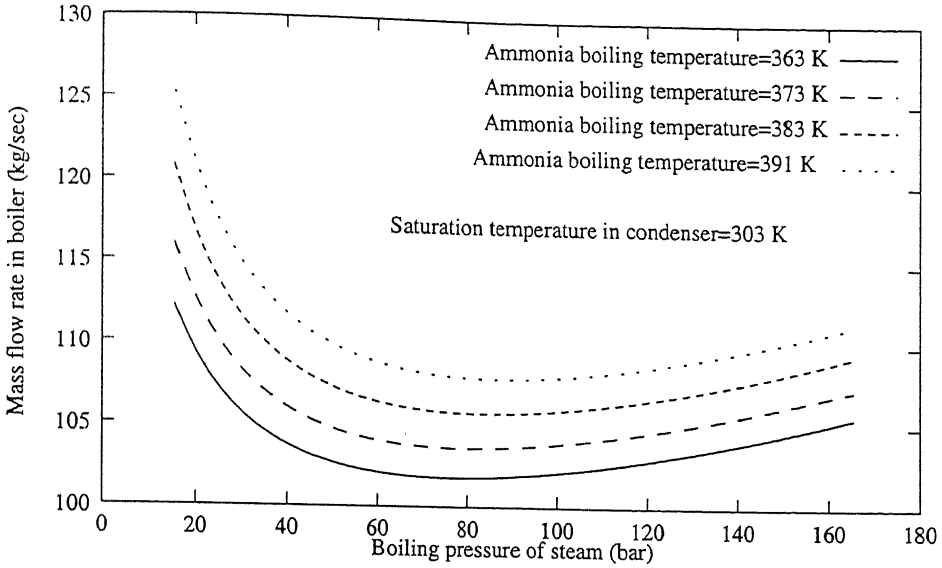

Figure 4.21: Variation in mass flow rate in boiler of binary-vapour cycle with two feed water heaters with boiling pressure of steam at the constant saturation temperature in condenser = 303 K

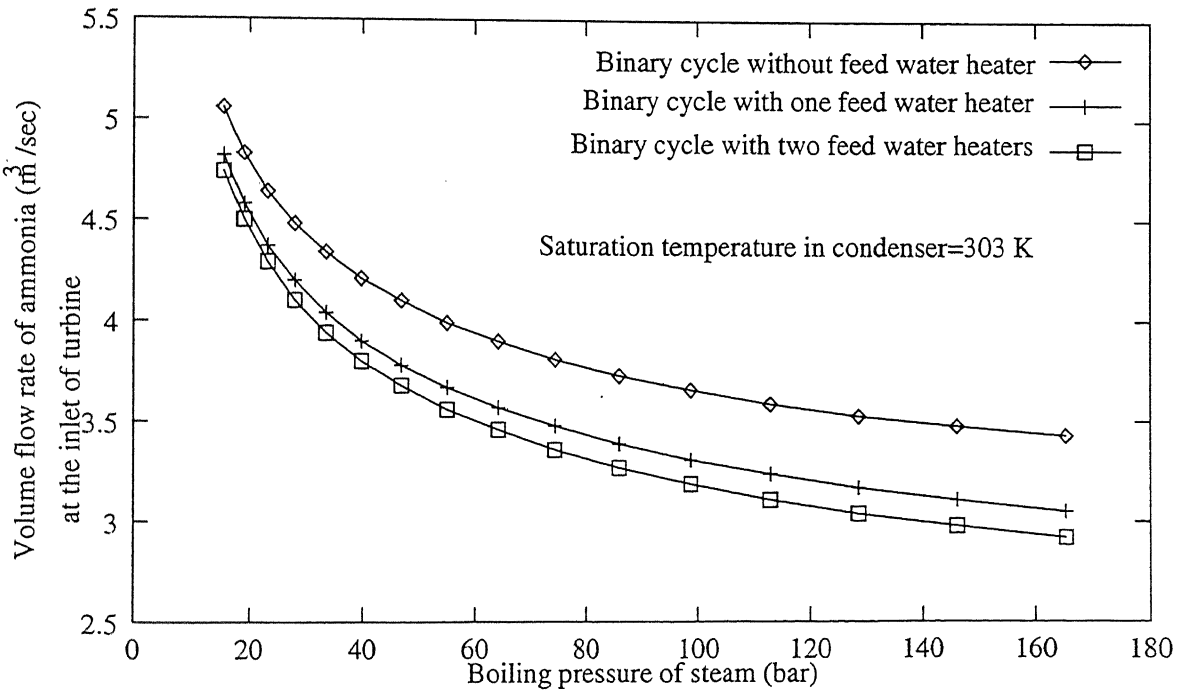

Figure 4.22: Variation in volume flow rate of ammonia with boiling pressure of steam at the constant saturation temperature in condenser =303 K

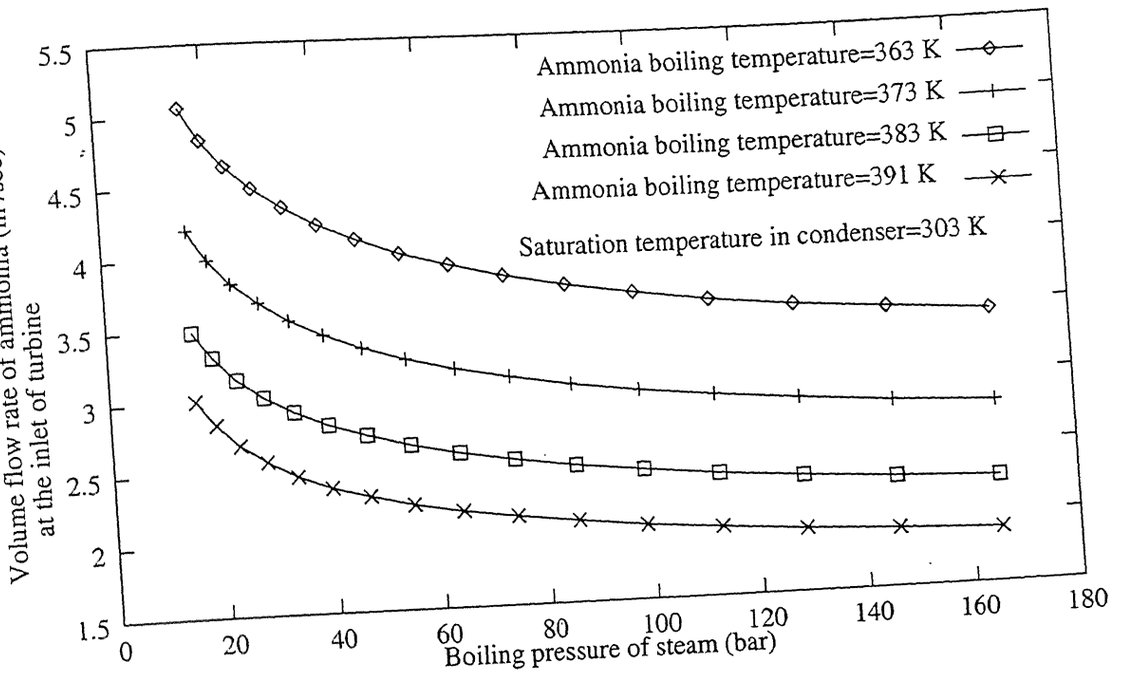

Figure 4.23: Variation in volume flow rate of ammonia of binary-vapour cycle without feed water heater with boiling pressure of steam at the constant saturation temperature in condenser $=303\,K$

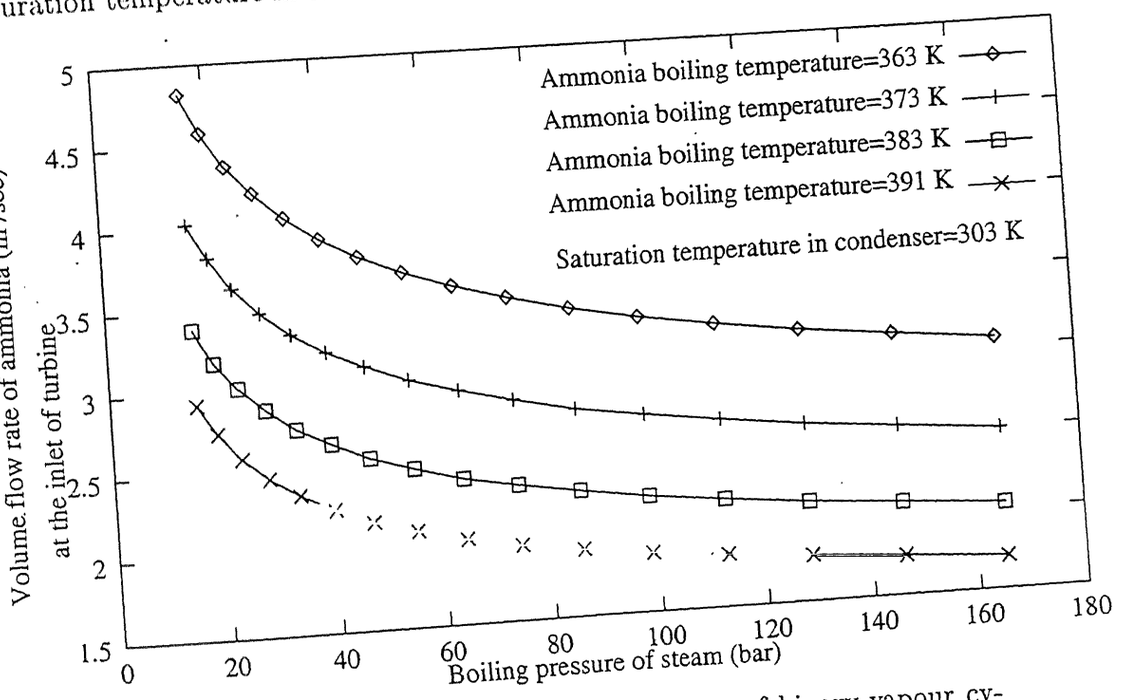

Figure 4.24: Variation in volume flow rate of ammonia of binary-vapour cycle with one feed water heater with boiling pressure of steam at the constant saturation temperature in condenser $=303\,K$

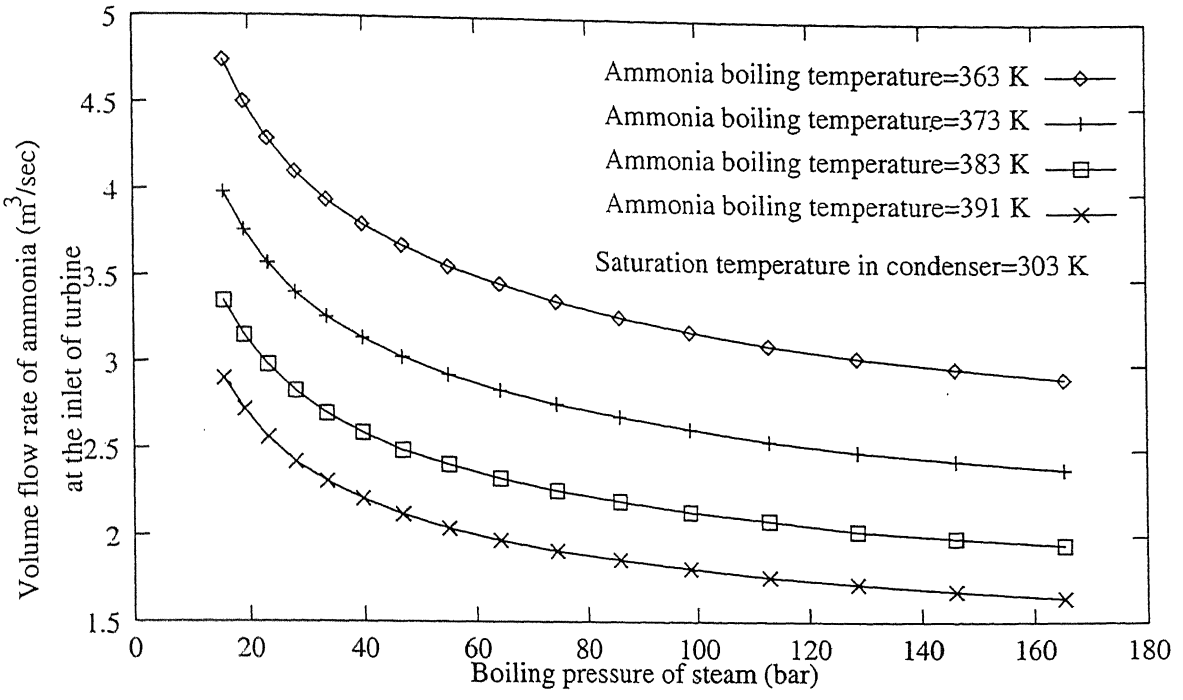

Figure 4.25: Variation in volume flow rate of ammonia of binary-vapour cycle with two feed water heaters with boiling pressure of steam at the constant saturation temperature in condenser $=303\,K$

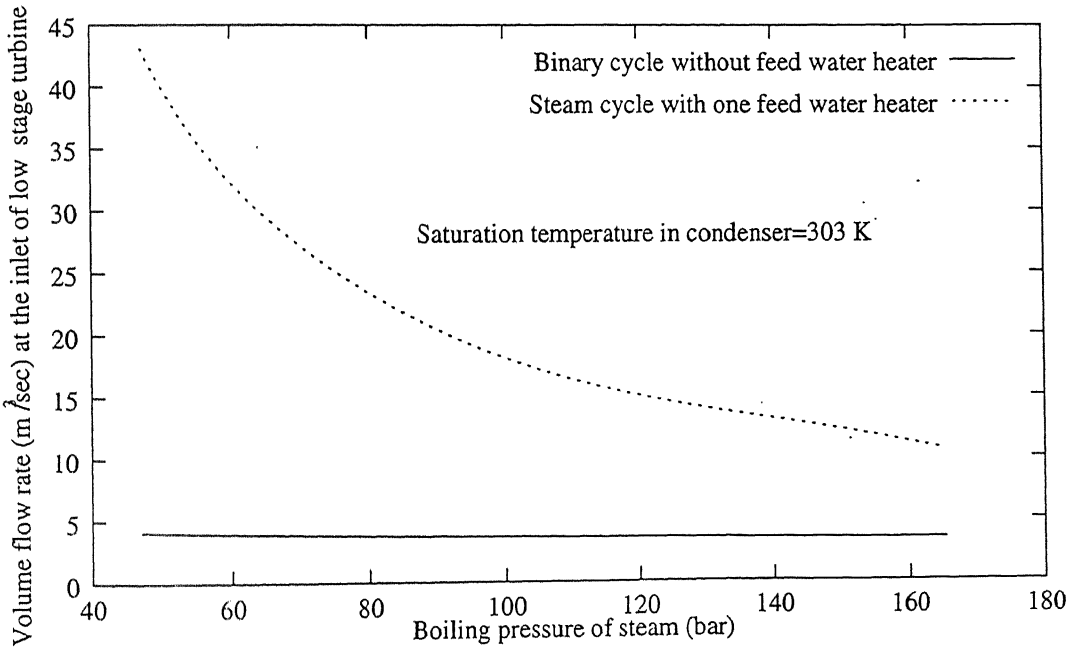

Figure 4.26: Variation in volume flow rate at the inlet of low stage turbine with boiling pressure of the steam at the constant saturation temperature in condenser $=303\,K$

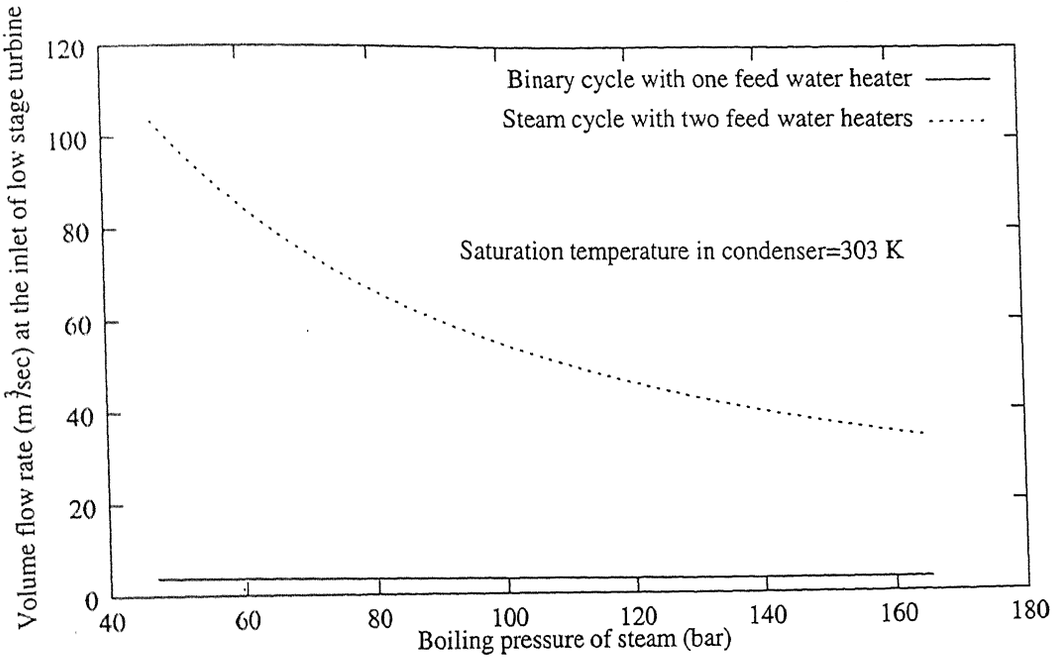

Figure 4.27: Variation in volume flow rate at the inlet of low stage turbine with boiling pressure of the steam at the constant saturation temperature in condenser=303 K

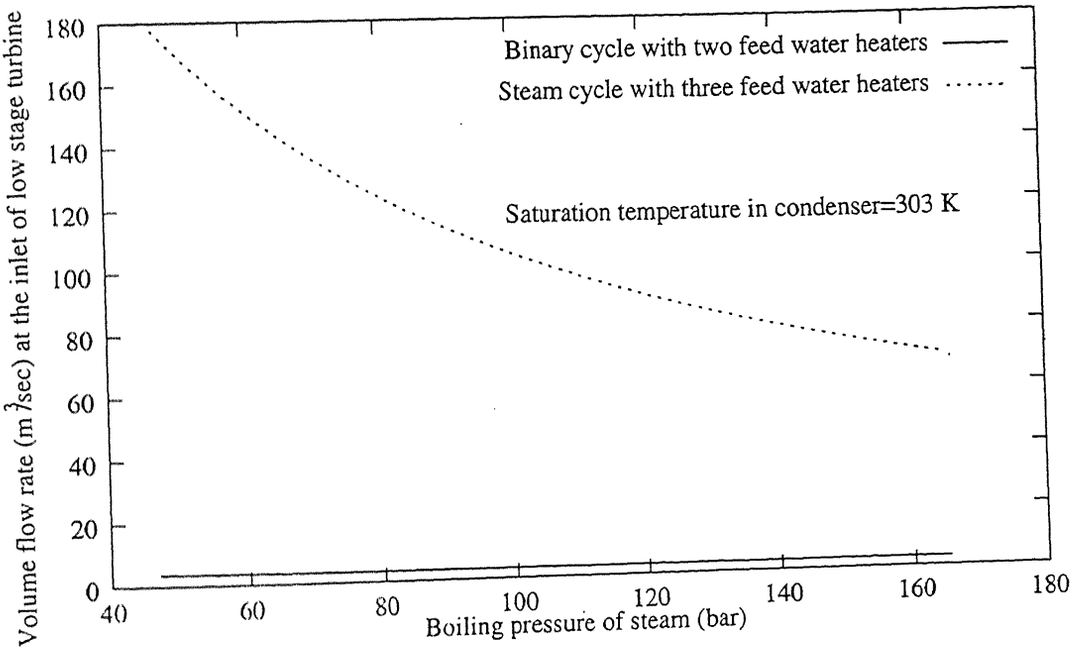

Figure 4.28: Variation in volume flow rate at the inlet of low stage turbine with boiling pressure of the steam at the constant saturation temperature in condenser=303 K

Chapter 5

Conclusions and Suggestions

5.1 Conclusions

The following conclusions are drawn from the present work :

1. Calculations have been carried out for a 100 MW power plant. In the topping cycle upto 3 feed waters heaters have been considered and the bottoming cycle has no feed heating.

2. Maximum efficiency for a steam cycle with one feed water heater occurs at the arithmetic mean of saturation tempeatures in boiler and condenser.

3. Efficiency of binary-vapour system is slightly less compared to steam cycle. Efficiency reduces as significant temperature difference between steam and ammonia is allowed.

4. Mass flow rate in condenser is much less in ammonia-water binary-vapour cycle than cycle using steam only.

5. Mass flow rate of ammonia decreases as number of feed water heaters are increased. Mass flow rate of ammonia decreases as boiling pressure of

steam increases.

6. At 165.4 bar boiler pressure, volume flow rate at the inlet and exit of the low-pressure turbine is 1/25 and 1/150, respectively in ammonia-water binary-vapour cycle than cycle using steam only.

7. At 165.4 bar boiler pressure, diameters at the inlet and exit of the low-pressure turbine is 1/5 and 1/12, respectively in ammonia-water binary-vapour cycle than cycle using steam only.

5.2 Suggestions

1. Effect of feed water heating in the ammonia side needs to be studied in order to see improvement in thermal efficiency of the binary system.

2. Economic analysis can be done for the ammonia-binary-vapour system to find out the initial investment, running cost though it can be intuitively concluded that same will be far less than the cost of system using steam only.

3. Pressure of feed water heaters for power plants running on ammonia binary-vapour system can be selected by using this computer programme.

Appendix A

Chebyshev Polynomials

Chebyshev polynomials are used for least square interpolation. Chebyshev polynomials are given by [5].

$$t_0 = 0.5 \tag{A.1}$$

$$t_1 = x \tag{A.2}$$

$$t_2 = 2x^2 - 1 \tag{A.3}$$

$$t_{n+1} = 2t_1 t_n - t_{n-1} \tag{A.4}$$

Appendix B

Thermodynamic Properties of Ammonia

B.1 Specific Volume of Saturated Liquid of Ammonia

Specific volume of saturated liquid of ammonia is given by [11].

$$v_f = \frac{1}{q_l} \tag{B.1}$$

$$q_l = q_c * [1 + \sum_{i=1}^{5} c_i (1 - \frac{T}{T_c})^{\frac{i}{3}}] \tag{B.2}$$

Where, v_f =specific volume of liquid (m^3/kg)

q_c =critical liquid density = $234.0\, kg/m^3$

q_l =density of saturated liquid (kg/m^3)

$c_1 = 1.615217$

$c_2 = 1.807593$

$c_3 = -1.401165$

$c_4 = 0.9919760$

c_5= -0.03569048

T=saturation temperature (K)

T_c =critical temperature = 405.50 K

B.2 Specific Volume of Saturated Vapour of Ammonia

$$v_g = \sum_{n=0}^{7} a_n * t_n(x) * 10^{-3} \qquad \text{(B.3)}$$

Where, v_g =specific volume of saturated vapour (m^3/kg)

t_n =Chebyshev polynomials

t_s =saturation temperature (°C)

	$0 \leq t_s < 60$	$60 \leq t_s \leq 120$
x	$\frac{t_s-30}{30}$	$\frac{t_s-90}{30}$
a_0	277.6908	53.3893
a_1	-113.6503	-18.8436
a_2	29.1961	3.1518
a_3	-6.02	-0.5403
a_4	1.0727	0.0509
a_5	-0.1726	-0.0118
a_6	0.0254	-0.0004
a_7	-0.0035	-0.0006

B.3 Entropy of Saturated Liquid of Ammonia

$$s_f = \sum_{n=0}^{7} a_n * t_n(x) \qquad \text{(B.4)}$$

Where, s_f =entropy of saturated liquid of ammonia (kJ/kg K)

t_n =Chebyshev polynomials

t_s =saturation temperature (°C)

	$0 \leq t_s < 60$	$60 \leq t_s \leq 120$
x	$\frac{t_s-30}{30}$	$\frac{t_s-90}{30}$
a_0	4.7461	6.6062
a_1	0.4632	0.4911
a_2	-0.00724	0.0243
a_3	0.0008	0.0079
a_4	0.0001	0.002
a_5	0.0	0.0006
a_6	0.0	0.0002
a_7	0.0	0.0001

B.4 Entropy of Saturated Vapour of Ammonia

$$s_g = \sum_{n=0}^{7} a_n * t_n(x) \tag{B.5}$$

Where, s_g =entropy of saturated vapour of ammonia (kJ/kg K)

t_n =Chebyshev polynomials

t_s =saturation temperature (°C)

	$0 \leq t_s < 60$	$60 \leq t_s \leq 120$
x	$\frac{t_s-30}{30}$	$\frac{t_s-90}{30}$
a_0	12.3488	11.0461
a_1	-0.3308	-0.3505
a_2	0.0118	-0.0272
a_3	-0.0016	-0.0092
a_4	0.0	-0.0024
a_5	0.0	-0.0007
a_6	0.0	-0.0002
a_7	0.0	-0.0001

B.5 Enthalpy of Saturated Liquid of Ammonia

$$h_f = \sum_{n=0}^{7} a_n * t_n(x) \tag{B.6}$$

	$0 \leq t_s < 60$	$60 \leq t_s \leq 120$
x	$\frac{t_s-30}{30}$	$\frac{t_s-90}{30}$
a_0	1128.7042	1766.23
a_1	142.0403	185.9883
a_2	1.6345	13.7632
a_3	0.2154	3.2727
a_4	0.0299	0.85
a_5	0.0019	0.2493
a_6	-0.0016	0.0756
a_7	-0.0026	0.0247

Where, h_f =enthalpy of saturated liquid of ammonia (kJ/kg)

t_n =Chebyshev polynomials

t_s =saturation temperature (°C)

B.6 Enthalpy of Saturated Vapour of Ammonia

$$h_g = \sum_{n=0}^{7} a_n * t_n(x) \tag{B.7}$$

Where, h_g =enthalpy of saturated vapour of ammonia (kJ/kg)

t_n =Chebyshev polynomials

t_s =saturation temperature (°C)

	$0 \leq t_s < 54$	$54 \leq t_s \leq 120$
x	$\frac{t_s-27}{27}$	$\frac{t_s-87}{33}$
a_0	3408.1289	3358.1124
a_1	15.8344	-53.4833
a_2	-3.5502	-19.7206
a_3	-0.1692	-4.2896
a_4	-0.0138	-1.2255
a_5	-0.0053	-0.3813
a_6	0.0	-0.1242
a_7	0.0	-0.0406

B.7 Saturation Pressure of Ammonia

Saturation pressure of ammonia is given by [11].

$$ln(\frac{p}{p_c}) = A + B(\frac{T}{Tc}) + \frac{C}{\frac{T}{Tc}} + D(\frac{T}{T_c})^2 + E(\frac{T}{T_c})^3 + \frac{F(1-\frac{T}{T_c})^{1.5}}{(\frac{T}{T_c})} \tag{B.8}$$

Where, p=saturation pressure (bar)

A=19.667984

B=-15.549930

C=-11.079219

D=9.114107

F=1.81269

T_c =critical temperature=405.50 K

p_c =critical pressure=113.53 bar

T=saturation temperature (K)

B.8 Enthalpy of Superheated Vapour of Ammonia

$$h_g = \sum_{n=0}^{7} c_n(y) * t_n(x) \tag{B.9}$$

$$y = \frac{t_s - 60}{60} \tag{B.10}$$

$$x = \frac{degsup - 90}{90} \tag{B.11}$$

$$c_n(y) = \sum_{m=0}^{7} b_m * t_m(y) \tag{B.12}$$

Where, h_g =enthalpy of superheated vapour of ammonia (kJ/kg)

t_s =saturation temperature (°C)

$degsup$ = degree of superheat (°C)

$t_n(x)$ =Chebyshev polynomials

$t_m(y)$ =Chebyshev polynomials

	c_0	c_1	c_2	c_3	c_4	c_5	c_6	c_7
b_0	7891.917	533.067	-28.3396	121548.7576	-44241.7932	18589.0214	-7980.04	5876.7
b_1	118.4331	62.6531	-16.6766	64371.2718	-28430.3465	13696.8698	-6405.1937	5056.64
b_2	-27.7705	11.4393	-5.0403	25641.5942	-14476.6787	8140.9864	-4169.38	3651.23
b_3	-3.9125	2.4247	-1.7067	10563.6417	-6933.6277	4324.8335	-2381.36	2301.39
b_4	-0.9412	0.7578	-0.0692	4239.3495	-3138.5855	2143.2862	-1260.83	1334.27
b_5	-0.311	0.2387	-0.2306	1664.5164	-1371.9216	1008.3361	-623.62	720.25
b_6	-0.1065	0.0801	-0.0875	653.8141	-578.16555	445.869	-294.19	361.09
b_7	-0.0427	0.0307	-0.0365	272.0216	-252.5554	209.4787	-139.78	187.36

B.9 Entropy of Superheated Vapour of Ammonia

$$s_g = \sum_{n=0}^{7} a_n(y) * t_n(x) * 10^{-5} \tag{B.13}$$

$$x = \frac{degsup - 90}{90} \tag{B.14}$$

$$a_n(y) = \sum_{m=0}^{7} b_m * t_m(y) \tag{B.15}$$

Where, s_g =entropy of superheated vapour of ammonia (kJ/kg K)

t_s =saturation temperature (°C)

$degsup$ = degree of superheat (°C)

$t_n(x)$ =Chebyshev polynomials

$t_m(y)$ =Chebyshev polynomials

	a_0	a_1	a_2	a_3	a_4
t_s	$0 \leq t_s \leq 120$	$18 \leq t_s \leq 120$	$0 \leq t_s \leq 120$	$0 \leq t_s \leq 120$	$0 \leq t_s \leq 66$
y	$\frac{t_s-60}{60}$	$\frac{t_s-69}{51}$	$\frac{t_s-60}{60}$	$\frac{t_s-60}{60}$	$\frac{t_s-33}{33}$
b_0	2634039.2858	128871.3092	-13627.0575	3795.1983	-547.0675
b_1	-107112.4378	6422.3971	-3485.8579	1553.5033	-120.9569
b_2	7493.0357	2014.5929	-1149.7532	609.5956	-25.3876
b_3	-2174.082	392.8705	-379.3708	248.7585	-96.813
b_4	-82.0241	126.0958	-147.5753	96.2697	-5.7800
b_5	-86.563	37.4694	-54.0439	37.2890	-4.0002
b_6	-25.6332	12.4024	-18.5529	18.6148	-2.4960
b_7	-11.1804	4.7725	-7.3680	8.7564	-1.4394

	a_4	a_5	a_5	a_6	a_7
t_s	$70 \leq t_s \leq 120$	$0 \leq t_s \leq 66$	$70 \leq t_s \leq 120$	$70 \leq t_s \leq 120$	$70 \leq t_s \leq 120$
y	$\frac{t_s-95}{25}$	$\frac{t_s-33}{33}$	$\frac{t_s-95}{25}$	$\frac{t_s-95}{25}$	$\frac{t_s-95}{25}$
b_0	-1964.0550	1467.8056	827.2694	-354.0112	255.0752
b_1	-726.4124	39.3903	394.6464	-198.2926	168.7846
b_2	-233.8985	10.0221	148.9912	-83.2312	82.2962
b_3	-69.6397	3.7600	49.6649	-30.0976	33.7420
b_4	-20.2421	2.1239	15.6666	-9.9786	12.5981
b_5	-6.0054	1.3134	4.8553	-3.1896	4.3869
b_6	-1.6103	0.8349	1.4854	-0.9729	1.4739
b_7	-0.5922	0.5966	0.4882	-0.1225	0.5743

t_s	a_1
0	59824.0811
6	59731.4234
12	59701.0446
18	59731.7476

t_s	a_4	a_5
66	-443.3623	131.4483
70	-435.1302	130.1301

t_s	a_6	a_7
0	-9.7159	2.884
6	-10.6687	3.078
12	-11.6208	3.3712
18	-12.7873	4.0379
24	-15.0987	4.0384
30	-15.8894	5.0300
36	-17.6511	5.5724
42	-19.7128	6.7977
48	-22.1636	7.8696
54	-25.7231	9.4115
60	-29.8201	11.1494
66	-20.5612	68.1460
70	-39.4898	16.4504

B.10 Specific Volume of Superheated Vapour of Ammonia

$$v_g = \sum_{n=0}^{7} p_n(y) * t_n(x) * 10^{-3} \tag{B.16}$$

$$x = \frac{degsup - 90}{90} \tag{B.17}$$

$$p_n(y) = \sum_{m=0}^{7} b_m * t_m(y) \tag{B.18}$$

Where, v_g =specific volume of superheated *vapour* of ammonia (m^3/kg)

t_s =saturation temperature (°C)

$degsup$ = degree of superheat

$t_n(x)$ =Chebyshev polynomials

$t_m(y)$ =Chebyshev polynomials

	p_0	p_1	$p_2(10^{-4})$	$p_2(10^{-4})$
t_s	$0 \leq t_s \leq 120$	$0 \leq t_s \leq 120$	$0 \leq t_s \leq 95$	$100 \leq t_s \leq 120$
y	$\frac{t_s-60}{60}$	$\frac{t_s-60}{60}$	$\frac{t_s-47.5}{47.5}$	$\frac{t_s-110}{10}$
b_0	537.829	76.3138	-28833.858	-20798.8
b_1	-329.0478	-43.6345	5949.7742	-466.3333
b_2	138.2894	18.8322	-1733.7865	-118.4286
b_3	-48.0197	-6.6411	220.1486	-11.6667
b_4	14.6213	2.0878	-50.0565	0.0
b_5	-4.0635	-0.5904	3.117	0.0
b_6	1.0371	0.1558	-1.575	0.0
b_7	-0.2494	-0.0375	-0.827	0.0

	$p_3(10^{-4}$	$p_3(10^{-4})$	$p_4(10^{-4})$	$p_4(10^{-4})$
t_s	$0 \leq t_s \leq 80$	$80 \leq t_s \leq 120$	$0 \leq t_s \leq 60$	$75 \leq t_s \leq 120$
y	$\frac{t_s-40}{40}$	$\frac{t_s-100}{20}$	$\frac{t_s-30}{30}$	$\frac{t_s-97.5}{22.5}$
b_0	7883.0203	6610.0180	-2127.9431	-2404.0019
b_1	-1463.3189	586.8857	319.6638	-485.1068
b_2	447.0288	193.5838	-85.2628	-155.0146
b_3	-49.6254	33.0	8.1725	-37.1587
b_4	11.3265	7.4414	-1.5568	-9.8119
b_5	-1.8048	1.3333	-0.1177	-1.5911
b_6	0.8015	-0.0356	0.2433	-1.1893
b_7	0.2764	-1.219	-0.2208	-0.1431

	$p_5(10^{-4})$	$p_5(10^{-4})$	$p_6(10^{-4})$	p_7
t_s	$0 \leq t_s \leq 42$	$75 \leq t_s \leq 120$	$75 \leq t_s \leq 120$	$75 \leq t_s \leq 120$
y	$\frac{t_s-21}{21}$	$\frac{t_s-97.5}{22.5}$	$\frac{t_s-97.5}{22.5}$	$\frac{t_s-97.5}{22.5}$
b_0	559.6989	991.3737	-417.4901	0.0290
b_1	-67.1546	313.8334	-170.5668	0.0155
b_2	12.7195	104.061	-61.4864	0.0065
b_3	-2.4791	28.5851	-17.9669	0.0023
b_4	-0.0423	8.5417	-5.0854	0.0007
b_5	0.7694	2.3931	-1.6757	0.0002
b_6	2.4734	1.2074	-0.1982	0.0
b_7	5.8643	t0.6985	-0.2964	0.0

t_s	p_2		t_s	p_4		t_s	p_5
95	-1.003		60	-0.0823		42	0.0232
100	-1.004		66	-0.0822		48	0.023
			70	-0.0822		54	0.0232
			75	-0.0844		60	0.0235
						66	0.0244
						70	0.0262
						75	0.0264

t_s	$p_6(10^{-4})$	p_7
0	-85	0.0024
6	-79	0.0021
12	-70	0.0023
18	-66	0.0020
24	-69	0.0024
30	-62	0.0021
36	-62	0.0020
42	-60	0.0021
48	-64	0.0023
54	-66	0.0022
60	-69	0.0026
66	-72	0.0031
70	-67	0.0040
75	-85	0.0037

Appendix C

Thermodynamic Properties of Steam

C.1 Enthalpy of Saturated Liquid

$$h_f = \sum_{n=0}^{7} a_n * t_n(x) * 0.1 \tag{C.1}$$

	$0 \leq t_s < 100$	$100 \leq t_s < 236$	$236 \leq t_s < 320$	$320 \leq t_s \leq 370$
x	$\frac{t_s-50}{50}$	$\frac{t_s-168}{68}$	$\frac{t_s-278}{42}$	$\frac{t_s-345}{25}$
a_0	4188.1623	14290.9635	24664.8121	33037.1912
a_1	2094.0919	2991.7219	2209.0742	2069.2907
a_2	1.31271	42.2673	70.2006	223.172
a_3	1.29107	5.929	8.5709	69.4128
a_4	-0.23937	0.609	1.2298	26.6501
a_5	0.11589	0.0659	0.2662	10.6612
a_6	-0.05306	-0.0214	0.0783	4.5517
a_7	0.00071	0.0056	0.1157	1.6313

Where, h_f =enthalpy of saturated liquid (kJ/kg)

t_n =Chebyshev polynomials

t_s =saturation temperature (°C)

C.2 Enthalpy of Saturated Vapour

$$h_g = \sum_{n=0}^{7} a_n * t_n(x) * 0.1 \tag{C.2}$$

Where, h_g =enthalpy of saturated vapour (kJ/kg)

t_n =Chebyshev polynomials

t_s =saturation temperature (°C)

	$0 \leq t_s < 100$	$100 \leq t_s < 236$	$236 \leq t_s < 320$	$320 \leq t_s \leq 370$
x	$\frac{t_s-50}{50}$	$\frac{t_s-168}{68}$	$\frac{t_s-278}{42}$	$\frac{t_s-345}{25}$
a_0	5179.77712	55063.222	55337.0687	51186.9596
a_1	87.71343	651.7661	-502.4306	-1712.0818
a_2	-1.59094	-135.4466	-151.6567	-395.1305
a_3	-0.22595	-13.8817	-16.6366	-113.7785
a_4	-0.01904	-0.3957	-2.17	-40.5655
a_5	-0.00160	0.2264	-0.1513	-16.1384
a_6	0.02274	0.2067	0.2591	-6.2431
a_7	0.01425	-0.0237	0.1843	-2.5004

C.3 Entropy of Saturated Liquid

$$s_f = \sum_{n=0}^{7} a_n * t_n(x) * 10^{-3} \tag{C.3}$$

Where, s_f =entropy of saturated liquid (kJ/kg K)

t_n =Chebyshev polynomials

t_s =saturation temperature (°C)

	$0 \leq t_s < 100$	$100 \leq t_s < 236$	$236 \leq t_s < 320$	$320 \leq t_s \leq 370$
x	$\frac{t_s-50}{50}$	$\frac{t_s-168}{68}$	$\frac{t_s-278}{42}$	$\frac{t_s-345}{25}$
a_0	1357.20862	4008.0589	6106.6591	7491.4305
a_1	651.77539	677.0974	390.6981	319.9379
a_2	-25.0617	-18.0248	3.7443	31.1037
a_3	1.71435	1.9342	1.3434	10.6539
a_4	-0.17464	-0.0679	0.0523	4.1465
a_5	0.06802	0.0275	-0.0342	1.6835
a_6	-0.01755	0.0272	-0.0450	0.5306
a_7	-0.00784	-0.0038	0.0031	0.2280

C.4 Entropy of Saturated Vapour

$$s_g = \sum_{n=0}^{7} a_n * t_n(x) * 10^{-3} \tag{C.4}$$

Where, s_g =entropy of saturated liquid (kJ/kg K)

t_n =Chebyshev polynomials

t_s =saturation temperature (°C)

	$0 \leq t_s < 100$	$100 \leq t_s < 236$	$236 \leq t_s < 320$	$320 \leq t_s \leq 370$
x	$\frac{t_s-50}{50}$	$\frac{t_s-168}{68}$	$\frac{t_s-278}{42}$	$\frac{t_s-345}{25}$
a_0	16328.7919	13444.9525	11725.5545	10454.1862
a_1	-892.0519	-585.0940	-314.9788	-350.0705
a_2	89.9277	39.9095	-9.5607	-55.0319
a_3	-8.1931	-6.9673	-2.7495	-17.1820
a_4	0.7776	0.6076	-0.3603	-6.0641
a_5	0.2214	-0.0264	-0.1970	-2.4713
a_6	-0.0997	-0.0900	0.1098	-1.0053
a_7	0.0214	0.0274	-0.0514	-0.2778

C.5 Specific Volume of Saturated Liquid

Specific volume of saturated liquid of steam is given by [12].

$$ln(\frac{v_c}{v_f}) = a11 * \tau^{\frac{1}{3}} + a12 * \tau^{\frac{2}{3}} + a13 * \tau + a14 * \tau^{\frac{7}{3}} + a15 * \tau^{\frac{8}{3}} \quad \text{(C.5)}$$

$$\tau = \frac{T_c}{T} - 1 \quad \text{(C.6)}$$

Where, $v_c = 0.003147\ (m^3/kg)$

v_f =specific volume of saturated liquid (m^3/kg)

a11=2.0198239

a12=-0.72813257

a13=-0.22418367

a14=0.20029413

a15=-0.13359233

T=saturation temperature (K)

T_c =critical temperature=647.27 K

C.6 Specific Volume of Saturated Vapour

Specific volume of saturated vapour of steam is given by [12].

$$v_g = v_{fg} + v_f \tag{C.7}$$

$$v_{fg} = \frac{z_{fg} * R * T * 0.001}{p_s} \tag{C.8}$$

$$ln(1 - z_{fg}) = a41 * \tau^{\frac{1}{3}} + a42 * \tau^{\frac{2}{3}} + a43 * \tau + a44 * \tau^{\frac{5}{3}} + a45 * \tau^3 + a46 * \tau^5 \tag{C.9}$$

$$\tau = \frac{T_c}{T} - 1 \tag{C.10}$$

Where, v_g =specific volume of saturated liquid (m^3/kg)

v_f =specific volume of saturated liquid (m^3/kg)

R=0.46151kJ/kgK

p_s =saturation pressure (MPa)

a41=-0.80915687

a42=-1.4874299

a43=-1.8106570

a44=-1.4309858

a45=0.041862761

a46=-0.046394800

T=saturation temperature (K)

T_c =critical temperature=647.27 K

C.7 Saturation Pressure

Saturation pressure of steam is given by [1].

$$log\, p = A + B log\, z + Cz + Dz \tag{C.11}$$

Where, p=saturation pressure (bar)

z=t+273.16=T+0.01

A=28.59051

B=-8.2

C=2.4804*10^{-3}

D=-3142.31

Equation C.11 is valid for the temperatures less than $100°C$.

$$log\, p = a + \frac{b}{z} + \frac{cx}{z}(10^{dx^2} - 1) + e10^{fy^{1.25}}$$

$$log\, p = a + \frac{b}{z} + \frac{cx}{z}(10^{dx^2} - 1) + e10^{fy^{1.25}} \tag{C.12}$$

Where, p=saturation pressure (bar)

x= $z^2 - g$

y=374.11-t

z=t+273.16=T+0.01

a=5.432368

b=-2.0051*10^3

c=1.3869*10^{-4}

d=1.1965*10^{-11}

e=-4.4000*10^{-3}

f=-5.7148*10^{-3}

g=2.9370*10^5

Equation C.12 is valid for the temperatures above $100°C$.

C.8 Superheated Properties for the Region $0°C \leq t \leq 350°C$

Superheated properties are given by [1].

$$v = \frac{RT}{p} + a_0(\Gamma)) + p\Gamma^6 a_1(\Gamma) + (p\Gamma^6)^4 a_2(\Gamma \tag{C.13}$$

Where, v=specific volume (cm^3/g)

R=4.6152 $bar\ cm^3/g\ deg\ K$

p=saturation pressure (bar)

T=saturation temperature (K)

$$\Gamma = \frac{500}{T} \tag{C.14}$$

$$a_0(\Gamma) = 0.512004 - 1.191807\Gamma + 2.599832\Gamma^2 - 21.433083\Gamma^3 + 15.281761\Gamma^4$$

$$-2.527165\Gamma^5 - 2.454047\Gamma^6 \tag{C.15}$$

$$a_1(\Gamma) = 0.661366 - 3.258346\Gamma + 6.393115\Gamma^2 - 6.447504\Gamma^3 + 3.202128\Gamma^4$$

$$-0.514945\Gamma^5 - 0.120192\Gamma^6 \tag{C.16}$$

$$a_2(\Gamma) * 10^6 = 8.44104 + 28.86344\Gamma - 270.10366\Gamma^2 + 624.08835\Gamma^3 - 675.70455\Gamma^4$$

$$+363.16788\Gamma^5 - 79.26405\Gamma^6 \tag{C.17}$$

$$h - h_0 = \frac{1}{10}\left\{p\left(a_0 + \Gamma\frac{da_0}{d\Gamma}\right) + \frac{1}{2}p^2\Gamma^6\left(7a_1 + \Gamma\frac{da_1}{d\Gamma}\right) + \frac{1}{5}p^5\Gamma^{24}\left(25a_2 + \Gamma\frac{da_2}{d\Gamma}\right)\right\} \tag{C.18}$$

$$h_0 = 1809.25 + 1.48286T + 3.79025 * 10^{-4}T + 46.174\, ln\, T \tag{C.19}$$

Where, h=enthalpy (KJ/kg)

$$\left(s + \frac{R}{10} ln\, p\right) - \left(s + \frac{R}{10} ln\, p\right)_0 = \frac{\Gamma}{5000}\left\{p\Gamma\frac{da_0}{d\Gamma} + \frac{1}{2}p^2\Gamma^6\left(6a_1 + \Gamma\frac{da_1}{d\Gamma}\right) + \right.$$

$$\left.\frac{1}{5}p^5\Gamma^{24}\left(24a_2 + \Gamma\frac{da_2}{d\Gamma}\right)\right\} \tag{C.20}$$

$$\left(s + \frac{R}{10} ln\, p\right)_0 = -1.5535 + 1.4286\, ln\, T + 7.58050 * 10^{-4}T - \frac{46.174}{T} \tag{C.21}$$

Where, s=entropy (KJ/kg K)

C.9 Superheated Properties for the Region $350°C \leq t \leq 500°C$

Superheated properties are given by [1].

$$W = \frac{p - RT\rho}{RT\rho^2} = B_8^T(y) * A^T * B_7(x) \tag{C.22}$$

Where, R=4.6152 $bar\, cm^3/g\, deg\, K$

p=saturation pressure (bar)

T=saturation temperature (K)

$\rho = density\, (g/cm^3)$

$$A = \begin{bmatrix} -2.933857 & -3.560472 & -0.752570 & -0.355238 & -0.171618 & -0.088253 & -0.023708 & -0.002024 \\ +2.178508 & +1.646874 & +0.257244 & -0.286577 & -0.191781 & -0.118835 & -0.020660 & 0 \\ -0.410626 & -0.712020 & -0.121860 & +0.067088 & +0.080874 & +0.014949 & 0 & 0 \\ +0.027044 & -0.046842 & -0.028628 & -0.032120 & -0.006524 & 0 & 0 & \\ +0.102056 & +0.134922 & +0.052882 & +0.007107 & 0 & 0 & 0 & 0 \\ -0.026332 & -0.049185 & -0.008993 & 0 & 0 & 0 & 0 & 0 \\ +0.002725 & +0.001175 & 0 & 0 & 0 & 0 & 0 & 0 \end{bmatrix}$$

$$x = \frac{\rho}{\rho_{max}} \tag{C.23}$$

$$y = \frac{\left(\frac{1}{T} - \frac{1}{T_{max}}\right)}{\left(\frac{1}{T_{min}} - \frac{1}{T_{max}}\right)} \tag{C.24}$$

$\rho_{max} = 0.70839\, g/cm^3$

$T_{min} = 468.15\, K$

$T_{max} = 1178.15\, K$

$$B_m(z) = \begin{bmatrix} b_1(z) \\ b_2(z) \\ \cdots\cdots\cdots \\ \\ \cdots\cdots\cdots \\ b_{m-1}(z) \\ b_m(z) \end{bmatrix} \tag{C.25}$$

$$= \begin{bmatrix} 1 \\ 2z - 1 \\ 2 * b_2 * b_2 - b_1 \\ 2 * b_2 * b_3 - b_2 \\ 2 * b_2 * b_4 - b_3 \\ \cdots\cdots\cdots\cdots\cdots\cdots \\ \cdots\cdots\cdots\cdots\cdots\cdots \\ 2 * b_2 * b_{m-1} - b_{m-2} \end{bmatrix} \tag{C.26}$$

$$\frac{h-h_0}{RT} = \frac{1}{10}\rho_{max}\left(xW + (y+\alpha)\int_0^x \frac{\partial W}{\partial y}dx\right) \tag{C.27}$$

$$h_0 = 1809.25 + 1.48286T + 3.79025 * 10^{-4}T + 46.174\, ln\, T \tag{C.28}$$

where, h=enthalpy (kJ/kg)

$$\alpha = \frac{\frac{1}{T_{max}}}{\left(\frac{1}{T_{min}} - \frac{1}{T_{max}}\right)} \tag{C.29}$$

$$\int_0^x \frac{\partial W}{\partial y}dx = B_8^T(x) * C_3 * A * B_8(y) \tag{C.30}$$

$$C_3 = \begin{bmatrix} \frac{1}{2} & -\frac{1}{8} & -\frac{1}{6} & \frac{1}{16} & -\frac{1}{30} & \frac{1}{48} & \frac{-1}{70} \\ \frac{1}{2} & 0 & -\frac{1}{4} & 0 & 0 & 0 & 0 \\ 0 & \frac{1}{8} & 0 & -\frac{1}{8} & 0 & 0 & 0 \\ 0 & 0 & \frac{1}{12} & 0 & -\frac{1}{12} & 0 & 0 \\ 0 & 0 & 0 & \frac{1}{16} & 0 & -\frac{1}{16} & 0 \\ 0 & 0 & 0 & 0 & \frac{1}{20} & 0 & -\frac{1}{20} \\ 0 & 0 & 0 & 0 & 0 & \frac{1}{24} & 0 \\ 0 & 0 & 0 & 0 & 0 & 0 & \frac{1}{28} \end{bmatrix} \tag{C.31}$$

$$\left(s + \frac{R}{10}ln\,\rho\right) - \left(s + \frac{R}{10}ln\,\rho\right)_0 = -\frac{1}{10}R\rho_{max}\int_0^x W\,dx + \frac{1}{10}R\rho_{max}(y+\alpha)\int_0^x \frac{\partial W}{\partial y}dx \tag{C.32}$$

$$\left(s + \frac{R}{10} ln\, \rho\right)_0 = -2.2593 + 1.02134\, ln\, T + 7.58050 * 10^{-4} T - \frac{46.174}{T} \quad \text{(C.33)}$$

where, s=entropy (kJ/kg K)

$$\int_0^x W dx = B_8^T(x) * C_3 * A * C_4 * B_7(y) \quad \text{(C.34)}$$

$$C_4 = \begin{bmatrix} 0 & 0 & 0 & 0 & 0 & 0 & 0 \\ 2 & 0 & 0 & 0 & 0 & 0 & 0 \\ 0 & 8 & 0 & 0 & 0 & 0 & 0 \\ 6 & 0 & 12 & 0 & 0 & 0 & 0 \\ 0 & 16 & 0 & 16 & 0 & 0 & 0 \\ 10 & 0 & 20 & 0 & 20 & 0 & 0 \\ 0 & 24 & 0 & 24 & 0 & 24 & 0 \\ 14 & 0 & 28 & 0 & 28 & 0 & 28 \end{bmatrix} \quad \text{(C.35)}$$

values of h, s, v are calculated from the equations C.27, C.32, C.23 respectively.

$$h(actual) = h(calculated) - \triangle h \quad \text{(C.36)}$$

$$s(actual) = s(calculated) - \triangle s \quad \text{(C.37)}$$

$$v(actual) = v(calculated) - \triangle v \quad \text{(C.38)}$$

values of $\triangle h$, $\triangle s$, $\triangle v$ are given in Tables C.1, C.2, C.3 respectively.

Table C.1: Values of Δh ($350°C \leq t \leq 500°C$)

Pressure	Temperature t ($°C$)														
(bar)	350	360	370	380	390	400	410	420	430	440	450	460	470	480	490	500
20	-5.7	-4.9	-4.1	-3.4	-2.8	-2.2	-1.6	-1.2	-0.8	-0.5	-0.3	-0.2	-0.1	0.0	0.0	0.0
40	-10.3	-9.0	-7.7	-6.5	-5.5	-4.5	-3.6	-2.8	-2.2	-1.7	-1.2	-0.8	-0.5	-0.2	0.0	0.0
60	-13.9	-12.2	-10.6	-9.1	-7.7	-6.4	-5.4	-4.4	-3.5	-2.7	-2.0	-1.4	-0.9	-0.4	-0.1	0.0
80	-16.3	-14.6	-12.8	-11.1	-9.5	-8.1	-6.8	-5.6	-4.5	-3.5	-2.6	-1.9	-1.1	-0.5	-0.2	0.0
100	-17.3	-16.0	-14.3	-12.6	-11.0	-9.5	-8.1	-6.7	-5.4	-4.2	-3.1	-2.2	-1.3	-0.6	-0.2	0.0
120	-15.8	-15.9	-14.9	-13.4	-11.9	-10.5	-9.0	-7.5	-6.1	-4.8	-3.7	-2.6	-1.6	-0.7	-0.2	0.0
140	-10.8	-13.3	-14.0	-13.4	-12.3	-11.1	-9.6	-8.0	-6.5	-5.3	-4.1	-2.9	-1.8	-0.8	-0.2	0.0
160	-0.5	-8.5	-12.0	-12.6	-12.1	-11.1	-9.8	-8.3	-6.9	-5.6	-4.3	-3.1	-1.9	-0.8	-0.2	0.0
180	14.3	3.0	-7.0	-10.7	-11.2	-10.8	-9.7	-8.3	-6.9	-5.6	-4.3	-3.1	-2.0	-0.9	-0.2	0.0
200	13.1	11.0	3.0	-7.0	-9.7	-9.9	-9.3	-8.1	-6.8	-5.5	-4.3	-3.1	-1.9	-0.8	-0.2	0.0
220	12.7	9.2	5.8	-2.9	-7.5	-8.2	-8.3	-7.5	-6.3	-5.1	-4.0	-2.9	-1.8	-0.8	-0.2	0.0

Table C.2: Values of Δs ($350°C \leq t \leq 500°C$)

Pressure	Temperature t ($°C$)															
(bar)	350	360	370	380	390	400	410	420	430	440	450	460	470	480	490	500
20	-0.009	-0.007	-0.006	-0.005	-0.004	-0.003	-0.002	-0.002	-0.001	-0.001	0.000	0.000	0.000	0.000	0	0
40	-0.015	-0.013	-0.011	-0.009	-0.008	-0.006	-0.005	-0.004	-0.003	-0.002	-0.002	-0.001	-0.001	0.000	0	0
60	-0.021	-0.018	-0.015	-0.013	-0.011	-0.009	-0.008	-0.006	-0.005	-0.004	-0.003	-0.002	-0.001	0.000	0	0
80	-0.024	-0.021	-0.019	-0.016	-0.014	-0.011	-0.010	-0.008	-0.006	-0.005	-0.004	-0.002	-0.002	-0.001	0	0
100	-0.025	-0.023	-0.021	-0.018	-0.016	-0.013	-0.011	-0.009	-0.007	-0.006	-0.004	-0.003	-0.002	-0.001	0	0
120	-0.023	-0.023	-0.021	-0.019	-0.017	-0.015	-0.012	-0.010	-0.008	-0.006	-0.005	-0.004	-0.002	-0.001	0	0
140	-0.015	-0.019	-0.020	-0.019	-0.017	-0.016	-0.013	-0.011	-0.009	-0.007	-0.006	-0.004	-0.002	-0.001	0	0
160	0.001	-0.011	-0.017	-0.018	-0.017	-0.016	-0.014	-0.011	-0.009	-0.008	-0.006	-0.004	-0.002	-0.001	0	0
180	0.024	0.006	-0.009	-0.015	-0.016	-0.015	-0.014	-0.011	-0.009	-0.008	-0.006	-0.004	-0.003	-0.001	0	0
200	0.022	0.018	0.006	-0.009	-0.014	-0.014	-0.013	-0.011	-0.009	-0.008	-0.006	-0.004	-0.002	-0.001	0	0
220	0.021	0.015	0.010	-0.003	-0.010	-0.011	-0.012	-0.010	-0.009	-0.007	-0.005	-0.004	-0.002	-0.001	0	0

Table C.3: Values of Δv ($350°C \leq t \leq 500°C$)

Pressure	Temperature t ($°C$)														
(bar)	350	360	370	380	390	400	410	420	430	440	450	460	470	480	490	500
20	-0.20	-0.16	-0.13	-0.11	-0.09	-0.07	-0.05	-0.04	-0.03	-0.02	-0.01	-0.01	0.00	0.0	0.0	0.0
40	-0.17	-0.14	-0.12	-0.10	-0.08	-0.06	-0.05	-0.04	-0.03	-0.02	-0.01	-0.01	0.00	0.0	0.0	0.0
60	-0.14	-0.12	-0.10	-0.08	-0.06	-0.05	-0.04	-0.03	-0.02	-0.02	-0.01	0.00	0.00	0.0	0.0	0.0
80	-0.11	-0.09	-0.08	-0.07	-0.05	-0.04	-0.03	-0.02	-0.02	-0.01	-0.01	0.00	0.00	0.0	0.0	0.0
100	-0.07	-0.07	-0.06	-0.05	-0.04	-0.04	-0.03	-0.02	-0.02	-0.01	-0.01	0.00	0.00	0.0	0.0	0.0
120	-0.011	-0.028	-0.035	-0.035	-0.031	-0.027	-0.022	-0.017	-0.013	-0.009	-0.006	-0.004	-0.001	0.0	0.0	0.0
140	0.054	0.012	-0.009	-0.016	-0.018	-0.016	-0.014	-0.011	-0.009	-0.006	-0.004	-0.002	-0.001	0.0	0.0	0.0
160	0.137	0.063	0.021	0.004	-0.04	-0.006	-0.006	-0.005	-0.004	-0.003	-0.002	-0.001	-0.001	0.0	0.0	0.0
180	0.048	0.143	0.063	0.027	0.012	0.005	0.002	0.001	0.001	0.00	0.00	0.00	0.00	0.0	0.0	0.0
200	0.040	0.050	0.123	0.056	0.032	0.018	0.012	0.008	0.005	0.004	0.002	0.001	0.00	0.0	0.0	0.0
220	0.033	0.038	0.051	0.057	0.044	0.029	0.020	0.014	0.010	0.006	0.004	0.002	0.001	0.0	0.0	0.0

C.10 Superheated Properties for the Region $500°C \leq t \leq 800°C$

superheated properties for the region $500°C \leq t \leq 800°C$ are calculated in a similar way [1] as given in section no. C.9, only difference is that here,

$\triangle h = 0$, $\triangle s = 0$, $\triangle v = 0$ and

$$A = \begin{bmatrix} -2.684145 & -3.110441 & -0.406137 & -0.143284 & -0.063656 & -0.048549 & -0.012639 & -0.000698 \\ +1.571884 & +0.553618 & -0.584342 & -0.801473 & -0.454050 & -0.215289 & 0 & 0 \\ -0.410626 & -0.712020 & -0.121860 & +0.067088 & +0.080874 & +0.014949 & 0 & 0 \\ +0.027044 & -0.046842 & -0.028628 & -0.032120 & -0.006524 & 0 & 0 & 0 \\ +0.102056 & +0.134992 & +0.052882 & +0.007107 & 0 & 0 & 0 & 0 \\ -0.026332 & -0.049185 & -0.008993 & 0 & 0 & 0 & 0 & 0 \\ +0.002775 & +0.001175 & 0 & 0 & 0 & 0 & 0 & 0 \end{bmatrix} \quad \text{(C.39)}$$

Bibliography

[1] Bain, R.W., *Steam Tables*, Her Majesty's Stationary Office, 1964

[2] El-Wakil, M. M., *Power Plant Technology*, McGraw-Hill Book Company, 1984

[3] Prasad, M., *Refrigeration and Air Conditioning Data Book*, Willey Eastern Ltd., 1987

[4] Kadambi, V. and Prasad, M., *An Introduction To Energy Conversion*, Volume I, Willey Eastern Ltd., 1976

[5] Jain, M. K., Iyenger, S. R. K., Jain, R. K., *Numerical Methods For Scientific & Engineering Computation*. Willey Eastern Ltd., 1993

[6] Kearton, W. J., *Steam Turbine Theory & Practice*, 1958

[7] Morse, F. T.. *Power Plant Engineering*, East-West Press Pvt. Ltd., 1964

[8] Nag, P. K., Engineering Thermodynamics, Tata McGraw-Hill Publishing Company Ltd., New Delhi, 1981

[9] Vasandani, V. P., Kumar D. S., Heat Engineering, Metropolitan Book Compaany Ltd., New Delhi, 1984

[10] Sorenson, Harry A., *Energy Conversion Systems*, John Willey & Sons, 1983

[11] *Thermodynamic and Physical Properties of Ammonia*, International Institute of Refrigeration, Paris, 1981

[12] Straub, J. and Schettler, K., *Water and Steam*, Pergamon Press, Germany, 1979, pp.150-157

[13] Potter, P. J., *Power Plant Theory and Design*, The Ronald Press Company, New York, 1959

[14] Keenan, J. H., *Steam Tables*, John Willey & Sons, 1983